# SYNAPTONEMAL COMPLEX AND RECOMBINATION NODULES IN WILD-TYPE *DROSOPHILA MELANOGASTER* FEMALES[1]

ADELAIDE T. C. CARPENTER

*Department of Biology, B-022, University of California, San Diego, La Jolla, California 92093*

Manuscript received October 18, 1978
Revised copy received January 3, 1979

ABSTRACT

Electron microscope serial section reconstruction analysis of all zygotene-pachytene nuclei of meiotic cells from three wild-type germaria (a subunit of the ovary containing the early meiotic stages arrayed in temporal developmental sequence) of *Drosophila melanogaster* females corroborates and extends earlier observations (CARPENTER 1975a) on the nature and sequence of ultrastructural events occurring during the time of meiotic recombination. Emphasis has been placed on (1) the time of appearance and disappearance of the synaptonemal complex (SC) and the changes in its dimensions that accompany a cell's progression through pachytene, and (2) the appearance, disappearance, number and chromosomal locations of recombination nodules (CARPENTER 1975b). For both the SC and the recombination nodule the availability of several developmental series has provided an estimate of the biological variability in the properties of these recombination-associated structures. The much more extensive data presented here substantiate the earlier hypothesis that recombination nodules occur at sites where reciprocal meiotic recombination will occur, has occurred, or is occurring. A second morphological type of recombination nodule is reported; it is suggested that the presence of the latter type of nodule may correlate with sites of gene conversion. The hypothesis that there may be two types of meiotic recombination processes is discussed.

CURRENTLY, electron microscopical investigations of events that accompany meiotic recombination are focused on two structures that are present during pachytene. The first of these is the synaptonemal complex (SC), a continuous tripartite structure present between the synapsed homologues of each bivalent at pachytene (see Figure 4). The presence and fine structure of the SC has been studied in a wide variety of forms (for reviews see MOSES 1968, 1969; WESTERGAARD and VON WETTSTEIN 1972; GILLIES 1975). Although a number of roles have been suggested for this structure, current consensus is that the SC itself is not directly involved in meiotic recombination, but rather most likely functions in meiotic synapsis and/or maintenance of the synaptic state. The second pachytene structure, the recombination nodule, is, however, a good candidate for a structure directly involved in the mediation of meiotic recombination. Its description in *Drosophila melanogaster* females, wherein the numbers, locations and

[1] Research supported by Public Health Service grants GM23338 and GM22231.

distributions of nodules could be shown to be nearly identical to those of meiotic recombination events, led to the suggestion that the recombination nodule at least marks the site of crossing over and to the hypothesis that the recombination nodule mediates some or all of the events during recombination (CARPENTER 1975b).

Recombination nodules have also been reported in: fungi (SCHRANTZ 1970; GILLIES 1972; ZICKLER 1973; RADU, STEINLAUF and KOLTIN 1974; H. FLETCHER, personal communication; CARMI *et al.* 1978), algae (STORMS and HASTINGS 1977), nematodes (BOGDANOV 1977; GOLDSTEIN and TRIANTAPHYLLOU 1978), rodents, lemurs, lemuroids and humans (MOSES, RUSSELL and CACHEIRO 1977; MOSES 1977a, b, and personal communication), male Bombyx and humans (RASMUSSEN, cited in GILLIES 1979); in those organisms where both the frequency and/or distribution of recombination events and of recombination nodules are known, they show striking parallels (Saccharomyces, BYERS and GOETSCH 1975; Sordaria, ZICKLER 1977, Rattus, MOENS 1978; Neurospora, GILLIES 1979).

This report is a continuation of a detailed electron microscopic (EM) analysis of the events of *D. melanogaster* female meiosis, initiated with the goal of detecting the presence and delineating the properties of ultrastructural components that may be involved in the processes of meiotic chromosome behavior. Particular attention is currently being focused on the properties of the SC and the recombination nodule. In two previous reports (CARPENTER 1975a, b), a complete EM reconstruction analysis of a series of wild-type nuclei (from a single germarium, thus in known developmental sequence) was presented. One drawback of the previous report was that since only one developmental time sequence of nuclei was completely analyzed, it was perforce impossible to obtain estimates of the biological variance in the properties of the SC and the recombination nodule. Consequently, three more developmental-time series of zygotene-mid-pachytene nuclei have been analyzed and are reported herein. This more extensive analysis of wild-type meiosis also provides a firm standard to which the ultrastructural effects of recombination-defective meiotic mutants can be compared. During this study, a second morphological type of recombination nodule was recognized; the two types of nodules differ somewhat in their properties. It is possible that the two types of nodules correspond to the two types of exchange—reciprocal and nonreciprocal (gene conversion).

## MATERIALS AND METHODS

*The organization of the Drosophila ovariole*: The Drosophila ovary is composed of a number of parallel ovarioles. Each ovariole is composed of two segments: the anterior germarium and the posterior vitellarium. At the anterior end of the germarium reside several stem cells; these give rise by mitosis to daughter stem cells, which remain at the anterior end, and to daughter cystoblast cells. The cystoblast undergoes four rounds of mitotic divisions, producing a cyst of 16 cells (cystocytes); these mitotic divisions involve incomplete cytokinesis, leaving cytoplasmic connections with a differentiated rim (ring canals) between daughter cells. Inheritance of pre-existing ring canals is determinate in the third and fourth rounds of mitosis, resulting (almost invariably) in a set pattern of connections among the 16 cells. Each 16-cell cyst moves (or is pushed) as a unit posteriorly through the germarium, acquires a layer of

follicle cells in the posterior region of the germarium, and passes on to the vitellarium, eventually to emerge from the fly as a mature egg.

Fifteen of the 16 cells will become nurse cells and perform nutritive roles in oogenesis; the remaining cell will become the oocyte. Choice of cell for oocyte is not random; only two of the 16 cells have four ring canals, and one of these becomes the oocyte. However, both cells with four ring canals enter meiosis, as evidenced by entry into pachytene (completion of formation of SC along bivalents), and acquire recombination nodules; at about the germarial-vitellarial juncture, one of the two cells loses its SC and reverts to a nuclear morphology similar to that of the other 14 nurse cells. At this time the oocyte is said to be determined.

New 16-cell cysts are produced at intervals and begin their posterior journey; the steady-state germarium thus contains a number of 16-cell cysts of differing ages. One of the advantages of Drosophila females in investigations of meiotic processes is that the germarial 16-cell cysts are in linear order, anterior to posterior, with respect to developmental age; thus, a survey of all cysts in one germarium presents a developmental series of known order. However, the developmental time differential between adjacent cysts cannot *a priori* be taken as constant, either within or between germaria.

For further details on ovariole organization see KING (1970), MAHOWALD and STRASSHEIM (1970), and CARPENTER (1975a).

*Fixation and reconstruction procedures*: Females were collected as virgins and held with males on yeasted food for two to three days to attain steady-state egg production. Ovaries were dissected from etherized females in insect Ringers, fixed (see CARPENTER 1975a for fixation and pre-stain procedure), and single ovarioles (germarium + first few vitellarial cysts) were flat-embedded in Epon 812-Araldite 6005. Subject to the vagaries of embedding, the planes of sectioning was perpendicular to the long axis of the germarium in order to minimize the number of sections; nevertheless, 300 to 500 consecutive sections are typically necessary to obtain a complete series. Sections (80 or 90 nm thick) were taken with a diamond knife on a Huxley-Cambridge microtome, picked up on formvar-coated loops, transferred to single-hole (2 × 1 mm) grids, stained with uranyl magnesium acetate at 37° for 90 min (FRASCA and PARKS 1965) and with lead citrate for six min at room temperature (REYNOLDS 1963), and carbon-coated under vacuum. Low magnification (various, but typically 800 to 1000×) micrographs were taken every six to ten sections, printed, and used to reconstruct the various cysts in the germarium by virtue of the ring canal connections (see CARPENTER 1975a); thus, the order of cysts was determined and the two cells with four ring canals—both potential oocytes—per cyst were identified. All nuclear sections of these potential (=pro) oocytes were then photographed at 10–12,000× (each nuclear series included a photograph of a calibration grid; each series was photographed, and subsequently printed, as a unit in order to maintain uniformity of magnification. Absolute magnification was calculated for each series from its calibration micrograph; final magnifications ranged from 30,000 to 35,000). Microscopes used during the course of this study included (in temporal order) a Philips 200, a JOEL JEM 100B, and a Zeiss EM 10A.

Nuclear reconstructions were performed from the prints in the following manner: the nuclear envelope outline and synaptonemal complex segments of each nuclear section were traced onto thin acetate sheets (one per print), the sheets were stacked using both nuclear membrane and SC for orientation, and the bivalent arms were followed (and color-coded). Tracings of each arm were made in which section numbers were noted at each change of pitch or direction of SC, then length of the SC of each such segment was measured (to the nearest mm) with thin copper wire. Length of the SC of each segment and, by summing segments, of each bivalent arm, was calculated as the hypoteneuse of a right triangle whose base is the measured projected length and whose height is the number of sections transversed by the segment, adjusted for the section thickness of the germarial series (as estimated by interference color of the sections) and the magnification factor of the particular nuclear series. Calculations were performed on a programmed HP-25 calculator.

Thickness of the SC was measured from the prints to the nearest 0.1 mm, using calipers. Thickness measurements (top to bottom of the central element) were taken only from segments clearly in sagittal section (see CARPENTER 1975a); all such sagittal views were measured. Raw

measurements were converted to nm, then mean and standard deviation were calculated using the inherent program of the HP-25 calculator.

Dimensions of recombination nodules were also measured to the nearest 0.1 mm by calipers from prints and converted to nm; plane of sectioning was determined by reference to the SC in the same, and adjacent, sections.

Genotypes of flies were as follows: block number A139 was from a *y pn cv nod*; $spa^{pol}$ female, block number A6 was from a *y*; $spa^{pol}$ female, and block number A294 was from a Canton-S female. The previously reported analysis, of block number A12, was also from a *y*; $spa^{pol}$ female and was from the same fixation series as A6; the other two are from separate fixation series. Canton-S is a wild-type strain; *y*, *pn*, *cv*, and $spa^{pol}$ are morphological markers (see LINDSLEY and GRELL 1968)—the *y*; $spa^{pol}$ strain has been studied as the control for the analysis of recombination-defective mutants (CARPENTER, in preparation) that carry the same morphological mutants, and *nod* (*no distributive disjunction*) is a meiotic mutant whose defect lies in the distributive system; recombination and disjuncton of elements that have undergone exchange are normal in its presence (CARPENTER 1973). Germarium A6 is unusual in the number of dead (cyst 8) and apparently dying (cysts 2 to 4) cysts; cells of cyst 8 are obviously necrotic, whereas cysts 2 to 4 are not. However, cysts 2 to 4 contain numerous lysosomes, only traces of synaptonemal complex (primarily in heterochromatic regions) and, for cyst 4, membranes across the ring canals. Apparently ring canal removal accompanies necrosis of a cyst—most of the cells in A6 cyst 8 are no longer connected by ring canals, and necrotic cysts in other germaria have consisted entirely of separate cells (see also RASMUSSEN 1975).

Since death of a cyst presumably reflects defectiveness incompatible with normal function, such a high frequency in one germarium suggests a systematic defect, perhaps a defective stem cell. Germarium A6 is also unusual in that among the apparently healthy cysts there are abnormally high numbers of bivalent juxtapositions—bivalents so close that their synaptonemal complexes form a polycomplex of two layers. There are no regularities of arm involvement such as would be expected from unsuspected heterozygosity for chromosomal aberrations and in most cases the polycomplex imparts no ambiguity to the reconstructions. Such polycomplexes are rare in other germaria.

## RESULTS

### *Gross germarial morphology*

Since information on the variability of proliferation and progression dynamics in wild-type germaria is essential for investigations of mutants potentially affecting such dynamics, and since the generality of some germarial phenomena has been questioned (DAY and GRELL 1976), the gross dynamics (features ascertainable from the low magnification photographs) of wild-type germaria are of interest. Various facets of germarial morphology have been reported from five wild-type germaria examined from serial sections at EM magnifications (KOCH and KING 1966; KOCH, SMITH and KING 1967; SMITH and KING 1968, one germarium; MAHOWALD and STRASSHEIM 1970, three germaria; RASMUSSEN 1974, one germarium); however, since each of these reports focuses on a different phenomenon, they do not provide a body of data from which it is possible to assess variability. I have now analyzed eight wild-type germaria sufficiently to determine gross morphological parameters; for four of these (CARPENTER 1975a and this report) complete serial section reconstruction was possible. For the other four germaria, total serial reconstruction was prevented by rupture of the supporting film of crucial grids or by incomplete sectioning; however, the data collected before grid loss are sufficient to determine the gross morphological

TABLE 1

*Numbers of cysts with the indicated number of cells in seven serially-sectioned wild-type germaria and gross cyst characteristics of four of them*

| Germarium | Cells per cyst 1 | 2 | 4 | 8 | 16 | Probable classification of 1- and 2-cell cysts |
|---|---|---|---|---|---|---|
| A54 | 0 | 5 | 1 | 0 | 10(1†) | (2s-cb, 3c-c) |
| A84 | 3 | 2 | 0 | 1 | 7 | (1s, 2cb, 1s-cb, 1c-c) |
| A287 | 3 | 2 | 1 | 1 | 8 | (2s, 1cb, 1s-cb, 1c-c) |
| A305 | 2 | 3 | 2 | 0 | 7 | (1s, 1cb, 3s-cb) |
| A139 | 4 | 1 | 1 | 1† | 8 | (2s, 2cb, 1s-cb) |
| A6 | 3 | 3 | 0 | 0 | 12(4†) | (2s, 1cb, 3c-c) |
| A294 | 4 | 3 | 1 | 1 | 4 | (1s, 3cb, 3c-c) |

| Germarium | A54 | | | A84 | | | A287 | | | A305 | | |
|---|---|---|---|---|---|---|---|---|---|---|---|---|
| 16-cell cyst number | SC4rc | SC3rc | op | SC4rc | SC3rc | op | SC4rc | SC3rc | op | SC4rc | SC3rc | op |
| 1 | —/— | —/— | — | —/— | —/— | — | —/— | —/— | — | t/t | —/— | — |
| 2 | t/t | —/— | — | | NP | | t/t | —/— | — | +/+ | t/t | — |
| 3 | +/+ | —/— | — | +/+ | t/t | — | +/+ | t/t | — | +/+ | +/t | + |
| 4 | +/+ | t/t | ? | +/+ | t/— | + | +/+ | t/t | — | +/+ | t?/— | + |
| 5 | +/+ | +/NP | + | +/+ | —/— | ++ | +/+ | t/t | — | +/+ | t?/— | + |
| 6 | +/+ | t/t | ++ | +/t* | —/— | ++ | +/+ | —/— | + | +/t | —/— | +++ |
| 7 | +/+ | —/— | ++ | +/t | —/— | +++ | +/t | —/— | ++ | +/— | —/— | +++ |
| 8 | +/+ | —/— | ++ | | | | +/NP | —/— | ++ | | | |
| 9 | necrotic | | | | | | | | | | | |
| 10 | +/— | —/— | +++ | | | | | | | | | |

Data are derived from low-magnification micrographs.

* Abnormal cyst; only 14 cells. The indicated "4-ring-canal" cell connects to only 3 cells (one with 4 ring canals, one with 3, and one with 1), as though the next to last mitotic division of this cell, and this cell only, failed to occur.

Abbreviations: s = stem cell, cb = cystoblast, s-cb = stem cell-cystoblast 2-cell cyst, c-c = cystocyte-cystocyte 2-cell cyst; † = dead or dying; SC = synaptonemal complex in the indicated cell, rc = ring canal; — = absent, t = traces, + = fully present, NP = not photographed; op = organellar passage, ++ = indicates detectable passage through the ring canal joining the two pro-oocytes as well as through the other canals.

The 16-cell cysts are numbered from anterior (#1, youngest) to posterior (oldest); the most posterior cyst in each germarium (= highest number) is the stage 1 cyst.

properties of their cysts. The numbers and types of cysts in the germaria I have analyzed completely, as well as those whose analysis was incomplete, are presented in Table 1 and representative low magnification micrographs are presented in Figure 1.

The number of stem cells per germarium cannot be determined with certainty, since there is no obvious morphological difference between presumptive stem cells (anterior-most cells) and obligate cystoblasts (single cells, not anterior), nor are the anterior-most cells conspicuously interdigitated with the anterior somatic cells. Moreover, the stem cell-cystoblast cell division appears to involve ring-canal formation (see also KOCH, SMITH and KING 1967); this ring canal, however, becomes (or is) longer and narrower than cystocyte-cystocyte ring canals, and apparently becomes closed off at one end by membrane and ring-canal material, permitting the eventual separation of the two cells. Thus, not only is

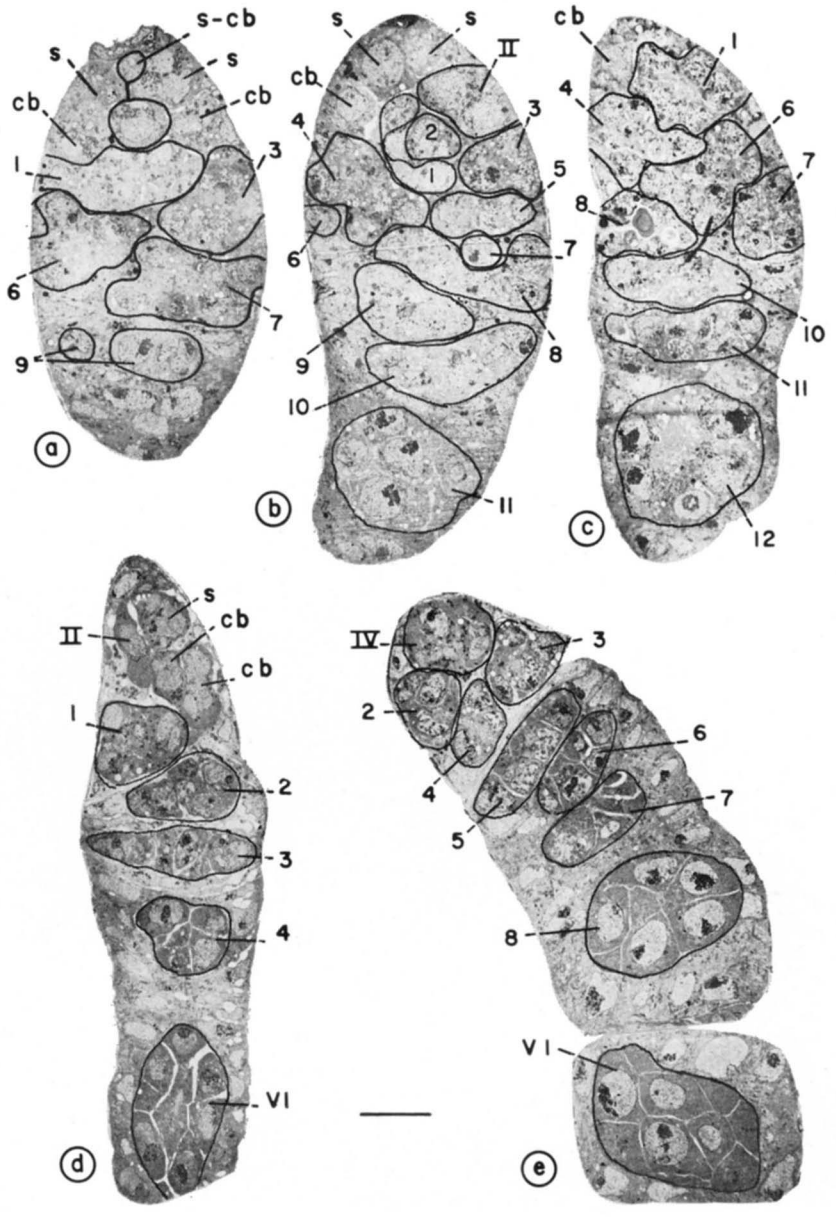


FIGURE 1.—Representative low magnification views of the four germaria indicating positions of the various cysts (outlined). (a, b) A12; (c) A6; (d) A294; (e) A139. s = presumptive stem cell, s-cb = presumptive stem cell-cystoblast pair, cb = cystoblast; II = 2-cell cyst, IV = 4-cell cyst; arabic numbers (1–12) indicate 16-cell cysts in anterior-posterior order (anterior is toward the top of the page); v1 = first vitellarial cyst (vitellarial designations, like germarial, indicate only relative position, not absolute stage). Magnification = 1,160x; bar = 10 $\mu$m.

the number of single cells an over-estimate of the number of stem cells—since some are cystoblasts—but also some of the apparent two-cystocyte cysts may rather be a stem cell-cystoblast association. For these reasons, the classifications of stem cells, cystoblasts and cystocytes for the one- and two-cell cysts presented in Table 1 are tentative (those cells in contact with the anterior osmophilic somatic cells are assumed to be stem cells). Nevertheless, the number of stem cells per germarium appears to vary—here, from one to four, with a mean of 2.6 (A12 appears to have had four stem cells); WIESCHAUS and SZABAD (1979) estimate 2.8 stem cells per ovariole from the frequency of mitotic recombination and clone size.

It is clear that there is substantial variation in the numbers of cysts at intermediate stages of the mitotic divisions and also in the number of germarial 16-cell cysts. For the latter, the numbers here range from four to 12; these data do not, however, represent a random sample, because longer germaria were preferentially chosen for sectioning since they yield more data (more cysts) per set of sections than do the shorter germaria.

Details of the gross morphology of the cysts in these germaria are given in Tables 1 and 2. The first (youngest) 16-cell cyst in a germarium typically contains no detectable SC and its nuclei are therefore in a pre-zygotene stage; the nuclei of four-ring-canal cells of the next 16-cell cyst typically contain some synaptonemal complex and are therefore in zygotene-pachytene. Although early zygotene nuclei are distinguishable from those in pachytene even at low magnifications by virtue of obviously fewer profiles of SC per section ("traces" in Table 1; confirmed for A287 and A305 by complete nuclear serial photography), late zygotene can be distinguished from pachytene only by serial reconstruction at high magnification (see below). In these eight germaria, there were seven pre-zygotene 16-cell cysts (germarium A12 had two such cysts; the younger had just completed the last mitosis—mid-body remnants were still present), three early zygotene cysts, three late zygotene cysts and three cysts in late zygotene or early pachytene. In contrast, there were 45 cysts in pachytene in these germaria. (The five necrotic or dying cysts and one incompletely sectioned cyst are excluded from this summary.) Since pachytene continues for some time after a cyst passes from the germarium into the vitellarium, a comparison of the numbers of pre-pachytene and germarial pachytene cysts overestimates the relative duration of the pre-pachytene stages. It is nevertheless clear that pre-pachytene stages are brief in Drosophila.

A major criterion by which the prophase stage of a meiocyte is determined at the EM level is the presence (or absence) and completeness of the synaptonemal complex. Before this criterion can be applied in Drosophila, it is also necessary to know that one is examining the two cells of the cyst that possess four ring canals, since one of these cells will become the oocyte. This is of concern because other cells in a cyst appear to enter meiosis transiently as indicated by the presence of at least some synapsed bivalent segments (condensed chromatin and SC). This phenomenon (entry into meiosis of a cell that is predestined not to complete it) is most clearly seen for the two three-ring canal cells (Tables 1 and 2; see also

TABLE 2

*Gross characteristics of the 16-cell cysts of the germaria A139, A6 and A294 and lengths (in μm) of synaptonemal complex (SC) from telomere to euchromatic-heterochromatic juncture. p = procentriole, † = necrotic or dying, Ex = extended, K = karyosome, np = not paired, ip = incompletely paired, i=short (≤ 1.5 μm) interruption in SC continuity, g=sub-telomeric X-chromosome gap, NP = not photographed, ph = photographed. Other symbols as in Table 1. Asterisks indicate footnotes which are listed by cyst/cell; parentheses indicate lack of identification. The letter designation that 4-ring canal cells acquired during germarial reconstruction has been retained; the letters and characteristics refer to cells with 4 ring canals with the sole exception of the "SC3rc" column which refers to the presence/absence of SC in the connecting cell with 3 ring canals. Vitellarial cysts are differentiated by the prefix "v"*

| Germarium Cyst/Cell | SC 4rc | SC 3rc | op | Centrioles‡ | # Sections‡ Total | # Sections‡ Missing | Length (μm) X | Bl | $A_2$ | $A_3$ | $A_4$ | T | # chromocenters |
|---|---|---|---|---|---|---|---|---|---|---|---|---|---|
| A139 1 f | - | - | - | | 28ph | | | | | | | | |
| a | - | - | | | NP | | | | | | | | |
| 2 i | + | + | - | 2+1p | 43 | 0 | 14.1g | 13.2i | 18.4 | 14.6 | 12.9i | 73.5 | 1(Ex) |
| a | + | t | | 1+1p | 68 | 0 | 15.4g | 12.7 | 17.9i | 13.1 | 12.2 | 71.3 | 1 |
| 4 a | + | t | - | 2+1p | 56 | 0 | 16.7 | 11.8 | 17.1 | 13.7 | 12.5 | 71.8 | 2 |
| i | + | + | | 2+1p | 64 | 1 | 16.2g | 11.6 | 14.6i | 14.3 | 11.9 | 68.6 | 1 |
| 3 i | + | t | - | 2 | 49 | 0 | 13.6 | 11.6 | 13.5 | 12.5 | 12.4* | 63.6 | 1 |
| a | + | t | | 2 | 58 | 0 | 13.2 | 13.5 | 13.5 | 11.8 | np | 52.0 | 3 |
| 5 i | + | - | + | ? | 44 | 0 | 11.1 | 7.8 | 11.0 | 9.8 | 9.7 | 49.4 | 1 |
| a | + | - | | 3+1p | 42 | 0 | 10.9 | 9.3 | 13.8 | 11.9 | 7.9 | 53.8 | 1 |
| 6 a | + | - | ++ | 1+1p | 48 | 1 | 8.2 | 7.6 | 8.5 | 7.8i | 6.4 | 38.5 | 1 |
| i | + | - | | 2+1p | 42 | 0 | 8.1 | 6.6 | 9.3 | 9.0 | 8.9 | 41.9 | 1 |
| 7 a | + | - | +++ | 6+3p | 40 | 0 | 10.8 | 8.3 | 10.0 | 9.6 | 7.5 | 46.2 | 1 |
| i | ±* | - | | 1+1p | 42 | 0 | 8.3 | 7.7 | 8.6 | 7.0 | ip | 31.6 | 1(EX) |
| 8 a | + | NP | +++ | 7+2p | 48 | 0 | 11.1g | 8.6-8.9 | 11.3 | 9.1 | 8.8 | 48.9-49.2 | 1 |
| i | - | NP | | | NP | | | | | | | | |
| v1 a | + | NP | +++ | ? | 20ph | 10 | | | | | | | |
| v2 a(K)*+ | | NP | +++ | ? | 53 | 0 | 9.8 | (10.4) | 11.1 | 9.2 | 7.5 | 48.0 | 1(Ex) |
| A6 1 e | + | - | - | 1 | 41 | 0 | 11.0?* | 11.6 | 15.7i | 10.9 | ip | 49.2 | 1 |
| i | + | - | | 2+1p | 48 | 0 | (13.0) | (9.5) | 9.1 | 8.7 | 16.7* | 57.0 | 1(Ex) |
| †2 g | - | - | - | 1 | 49 | 0 | | | | | | | |
| e | - | - | | 1+1p | 63 | 0 | | | | | | | |
| †3 c | - | - | - | 2 | 37 | 0 | | | | | | | |
| f | - | - | | 2 | 39 | 0 | | | | | | | |
| †4 j | - | - | - | 1 | 47 | 1,1,1 | | | | | | | |
| f | - | - | | 2 | 49 | 0 | | | | | | | |
| 5 d | + | + | - | 2+1p | 43 | 0 | 14.5 | 10.6 | 14.1 | 11.7 | 10.6 | 61.5* | 1(Ex) |
| c | + | + | | 1 | 59 | 1,1 | 10.9 | 9.4 | 11.2 | 10.0 | 10.5* | 52.0 | 1(EX) |
| 6 d | + | t | + | 1 | 47 | 0 | 10.9* | 9.3 | 12.8 | 10.2 | 10.1 | 53.3 | 2 |
| i | + | t | | 1+1p | 44 | 0 | 10.0 | 6.4 | 12.4 | 11.9 | 9.4 | 50.1* | 1 |
| 7 c | + | - | + | 1 | 36 | 0 | 7.9 | 6.7 | ip | ip | ip | 14.6 | 2 |
| i | + | - | | 16 | 45 | 1 | 9.2 | 9.2 | 13.4 | 10.7 | 8.8 | 51.3 | 1 |
| †8 | necrotic, no synaptonemal complex | | | | | | | | | | | | |
| 9 c | + | - | ++ | 1 | 45 | 1,2 | 10.0 | 9.0 | 11.7 | 9.7 | 9.2 | 49.6 | 1(Ex) |
| i | + | - | | >11+3p | 43 | 1 | 9.7 | 7.2 | 5.8 | 15.4* | | 38.1 | 1 |
| 10 c | + | - | +++ | 0 | 46 | 0 | 10.2 | 13.0 | 11.2 | 7.1* | 6.0* | 47.5 | 1 |
| i | + | - | | >13+2p | 51 | 0 | 8.2 | (7.4) | 13.0 | 10.2 | 8.1 | 46.9 | 2 |
| 11 e | + | - | +++ | 19+2p | 61 | 0 | 12.3 | 11.3 | 14.6 | 14.5 | 10.4 | 63.6 | 3 |
| i | t | - | | 0 | 51 | 1 | | | | | | | |
| 12 a(K) | + | - | +++ | 13+1p | 46 | 1 | 14.0 | (11.8) | 12.4 | 12.3 | 13.4* | 63.9 | 2 |
| A294 1 e | - | - | - | | NP | | | | | | | | |
| h | - | - | | | NP | | | | | | | | |
| 2 e | + | t | - | 2+1p | 63 | 0 | 13.5 | 12.3 | 16.5 | 14.8 | 12.7 | 69.8 | 1 |
| h | + | t | | 2 | 66 | 0 | 13.8g | 11.9 | 16.4i | 15.2 | 13.1 | 70.4 | 1 |
| 3 i | + | t | - | 1+1p | 56 | 0 | 11.2g | 10.6 | 14.3 | 12.4 | 11.8 | 60.3 | 2 |
| e | + | t | | 2+1p | 58 | 0 | (8.1)* | 13.2 | 15.9 | 12.8 | 11.5 | 61.5 | 1 |
| 4 i | + | - | + | 0 | 54 | 0 | 8.0 | 6.7 | 10.5 | 7.7 | 7.3 | 40.2 | 2 |
| e | + | - | | 1+1p | 53 | 0 | 8.1* | 8.1 | 11.6 | 8.6 | ip | 36.4 | 2 |
| v1 e | + | NP | ++ | 0 | 47 | 2 | 7.9 | 7.0 | 8.2 | 8.2i | 6.3i | 37.6 | 2 |
| i | + | NP | | 2 | 33 | 0 | 8.8g | 7.4 | 8.3 | 15.4* | | 39.9 | 1 |

‡ Since consecutive high magnification photographs were taken only through the serial extent of the nucleus, portions of the cytoplasm were not examined; therefore, the number of centrioles observed may be an underestimate.

* A139 3iA4: SC forks near telomere.
7i: to nurse cell.
v2a: early karyosome. The nucleolus has become the endobody and the blob is dissociated from its bivalent; hence, the blob autosome cannot be distinguished.
A6 1e: identity of X uncertain.

CARPENTER 1975a; RASMUSSEN 1974); these nuclei have exhibited SC in some cysts of all wild-type germaria examined. These nuclei first exhibit SC at or after the time that the nuclei of the four-ring-canal cells (pro-oocytes) have entered pachytene and the three-ring-canal cells no longer exhibit SC shortly thereafter; thus, entry into meiosis is transient for these nuclei. During this time, however, SC may be as extensively present in these nuclei as it is in pachytene nuclei of the four-ring-canal cells. Traces of SC have been observed in nuclei of two, and even of one, ring-canal cells. Clearly, the detection of SC within a nucleus does not necessarily imply that the nucleus is one of the two pro-oocytes (*contra* DAY and GRELL 1976). Whether the transient entry of obligate pro-nurse cells into meiosis performs some function or is simply a reflection of the cytoplasmic continuity between the 16 cells is moot. In *Bombyx mori* females this phenomenon is even more dramatic: all seven pro-nurse cells attain full pachytene (RASMUSSEN 1976).

An additional cyst characteristic recognizable at low magnification is the passage of organelles from nurse cells to the oocyte (Tables 1 and 2). Organellar passage is detected by the presence of mitochondria and A-bodies (KING 1970) within ring-canal lumens and their accumulation in the (pro)oocyte(s); at its initiation the number of organelles actually traversing the ring canal at the time of fixation may be low, but its occurrence is verified by mitochondrial location and morphology. Before organellar passage begins, the mitochondria are scattered throughout the cytoplasm and are relatively rounded; after organellar passage has begun, mitochondria of the obligate nurse cells are oriented toward, and through, the ring canals leading to the pro-oocytes and are elongated in the direction of apparent motion (see Figure 4a). Organellar passage between the two pro-oocytes is typically delayed one cyst relative to organellar passage from obligate nurse cells; this passage may, however, be evident before it is obvious which pro-oocyte will become the definitive oocyte as judged by either SC

---

1i: identity of X and blob-arm uncertain. SC in fragments; the 3 smallest (8.7, 3.3, 2.7) are summed as "A4".
5c: "A3", "A4", and a fragment form a 3-way juncture; the length of the fragment (2.3) has been added to that of A4 (8.2).
5d: 4 regions of polycomplex: 2 within A4, one between telomere of Bl chromosome and the blob itself, and one 6-way polycomplex involving the Bl arm twice and A4 once.
6d: A4 branched in two places: one such branch merges with X, making the total length of the X ambiguous.
6i: 3 regions of polycomplex: Bl arm—A3, a loop in X and a hairpin in A4; and the tip of A3 makes a Y-junction with the middle of the X.
9i: A3 and A4 telomeres abut—point of juncture indeterminate.
10c: telomeres of A3 and A4 nearly abut; A3 and A4 may be only one arm, with the remaining arm unpaired.
12a: "A4" = 9.6 $\mu$m chromocentral piece + a 3.8 $\mu$m fragment which is either the distal part of A4 or of X.
A294 3e: identity of X unclear. Heterochromatic SC from A2 and A3 also enter the nucleolus.
4e: SC of X splits into 2 at euchromatic-heterochromatic juncture; both branches enter and pass through nucleolus. Lengths of the 2 branches are equal to and through the nucleolus. Both branches have typical trilaminar SC.
v1i: A3 and A4 telomeres abut.

morphology/presence or apparent direction of organellar passage through the common ring canal.

A final gross morphological characteristic of cysts, and one that identifies which of the four ring-canal cells is determined to become the oocyte, is the disappearance of the SC from one of the four-ring-canal cells (Tables 1 and 2).

The cysts in these eight germaria, therefore, show an orderly progression of developmental events, from pre-zygotene to oocyte determination; typically (6 of 8) the first (most anterior) 16-cell cyst is not yet in zygotene, and the last germarial cyst (stage 1) has typically (7 of 8) attained oocyte determination. My previous finding (CARPENTER 1975a) that the intervening cysts are also arrayed according to their relative developmental ages is supported at the gross level by the orderly progressions of transient SC in nuclei of three-ring-canal cells and of organellar passage and is confirmed from detailed considerations of SC behavior (see below). It should be noted, however, that comparisons between germaria indicate that cysts of equivalent developmental ages are frequently not at the same absolute germarial position; absolute germarial position is, therefore, at best only a rough guide to the developmental stage of an individual cyst.

*Synaptonemal complex*

*Chromocentral organization*: As noted previously (CARPENTER 1975a), the pachytene bivalents typically have a chromocentral organization—the centromeres and centric heterochromatin of the four bivalents are frequently all in one region of the nucleus. However, the degree of proximity of the centromeric regions varies between nuclei. In some nuclei the centromeric regions of all 5 major chromosome arms (*X, 2L, 2R, 3L, 3R*) are so close that unambiguous reconstruction of the bivalents through the chromocenter is impossible; conversely, occasionally the three major bivalents are completely separate throughout. Numbers of chromocenters for the various nuclei are indicated in Table 2; 31% (11/36) have one or more major bivalents unassociated with the rest. Although the observation of such a high frequency of "split" chromocenters does not invalidate the hypothesis that the "pairing" aspect of the distributive system is mediated *via* chromocentral associations (NOVITSKI 1964), it does necessitate additional assumptions and therefore decreases the simplistic charm of that hypothesis.

*Discontinuities in synaptonemal complex*: Zygotene appears to be a relatively brief stage; there is at most one zygotene cyst in each of the wild-type germaria examined to date. The synaptonemal complex at zygotene is (by definition) discontinuous, but it is also extremely thin (see Figure 3); the chromatin in synapsed segments is typically less condensed than it is in pachytene nuclei in the same germarium, and in unsynapsed segments it is usually not condensed at all, nor are lateral (axial) elements evident. (Absolute degree of chromatin condensation throughout the germarium is a function of fixation conditions). Although direct comparisons between the adult steady-state germarium and the developing pupal germarium are premature, it is necessary to note that the conclusion of DAY and GRELL (1976) that zygotene in the pupal germarium is lengthy is based on inadequate and nonrepresentative data (total length of SC

per nucleus cannot be reliably extrapolated from measurements of only four sections, and comparisons of extrapolations from peripheral nuclear sections with those from central nuclear sections are meaningless).

Pachytene is operationally defined as starting at the completion of SC formation. However, this does not mean that all regions are invariably paired at pachytene.

Occasionally, short interruptions in SC continuity persist through pachytene (Table 2), and even more rarely there is complete or nearly complete failure of synapsis of an entire arm. The frequency of such complete or nearly complete failure (five instances out of 35 nuclei, or about 3% per arm) is much lower than the frequency of absence of exchange ($E_0$ tetrads: for the $X$ chromosome, $E_0 =$ 5%; for the autosomes, $E_0 = 10$ to 20% per arm), and therefore, in Drosophila (unlike maize, MAGUIRE 1972), synapsis and exchange are not absolutely correlated.

The occasional short interruptions on the autosomal arms show no evidence of consistency in arm or location. The interruptions on the $X$ chromosome, however, show striking consistency in location: they are all very near the distal end. The eight $X$ chromosome bivalents showing the distal interruption had an average of 0.7 $\mu$m of SC distal to the interruption (5% of total length), and the interruption itself averaged 0.8 $\mu$m (6% of total length). Since in these bivalents there must have been a site of synaptic initiation distal to the interruption, then if crossover-site determination presages synaptic initiation (MAGUIRE 1972), the relative frequency of exchange in the very distal portion of the $X$ chromosome should be high. Instead, it is very low (LINDSLEY and SANDLER 1977) and, interestingly, the telomeric depression in exchange also affects 10% of total (physical) length of euchromatin, suggesting that the frequent failure of complete synapsis in some way inhibits distal exchange.

Disappearance of synaptonemal complex in the four-ring-canal cell that is the pro-nurse cell is the reverse of synaptonemal complex formation in zygotene; the complex becomes progressively thinner, the chromatin less condensed, and intercalary interruptions—one to several per arm—in SC and chromatin continuity appear. Disappearance of SC in the oocyte has not yet been examined extensively; however, it occurs while the chromatin remains in the highly condensed karyosome stage (see also KING 1970), and hence, in Drosophila females, SC disappearance in the oocyte is not accompanied by desynapsis of homologues.

*Changes in SC dimensions during pachytene*: At pachytene, the synaptonemal complex is continuous along the arms (with exceptions noted above); therefore, the meanderings of the bivalents can be reconstructed by following the SC in serial photographs. As noted previously (CARPENTER 1975a), the SC (and hence the bivalents) undergo changes in length and thickness that correlate with relative position of germarial cysts and therefore appear to present a developmental sequence of zygotene-pachytene events. Observations from complete nuclear reconstructions of three additional germaria confirm this sequence.

In order to examine whether cysts are arrayed in a developmental sequence, it is necessary to determine their physical order in the germaria. In many

germaria, all cysts are in linear array so that order is unambiguous. However, the temporal order of 16-cell cysts can be ambiguous in the anterior part of the germarium (KING's region 1, KING 1970) since here there may be two or more (in A12, four) cysts abreast. Numerical order is assigned from careful consideration of cyst position in the low magnification photographs, but some assignments are of necessity arbitrary. In germarium A12, cysts 3 and 4 were arbitrarily ordered; in A139, cysts 3 and 4. Reconstruction of the SC in these two cases suggest that in both cases the arbitrary order is the inverse of the temporal order. As noted (CARPENTER 1975a), the synaptonemal complex in A12 cyst 4 contains interruptions and the cells are therefore probably in late zygotene; the synaptonemal complex in cyst 3 is continuous and the cells are therefore in pachytene. A12 cyst 5 is clearly farther down the garmarium than are cysts 3 and 4; the temporal order is therefore 2, 4, 3, 5. For A139, the zygotene cyst 2 is clearly anterior to cysts 3 and 4, which are in turn anterior to cyst 5; a smooth progression of length changes results from reversing the arbitrary order of cysts 3 and 4, suggesting that here too the temporal order is 2, 4, 3, 5.

To examine the dimensional changes that occur in the synaptonemal complex during pachytene, the lengths of the synaptonemal complex from telomere to the euchromatic-heterochromatic junction have been calculated for all five major

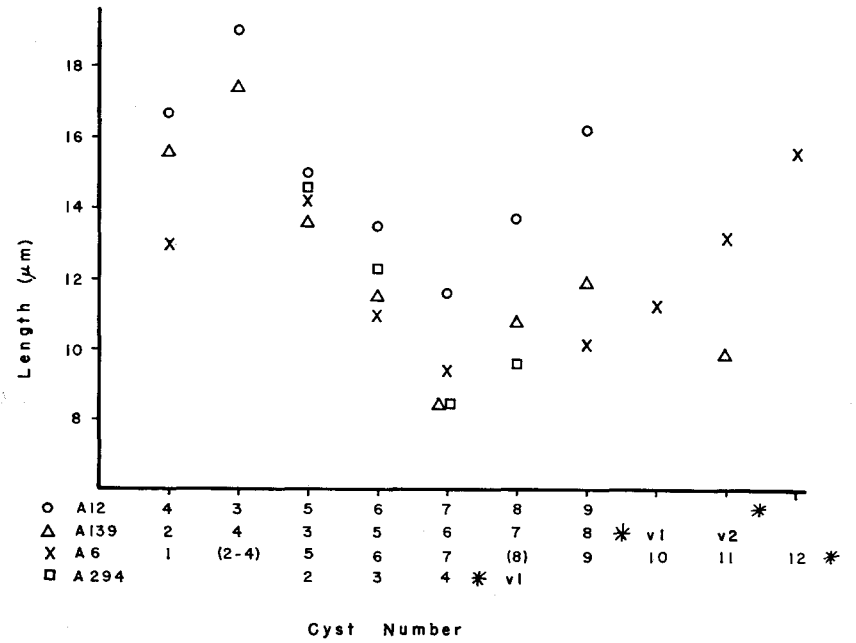


FIGURE 2.—Length of the *X*-chromosome bivalent as a function of developmental age of cyst. The *X* chromosome synaptonemal complex is measured from telomere to point of entry into nucleolus; where values are available from both cells with four ring canals, the average is presented. Cyst numbering begins with the anterior-most (youngest) 16-cell cyst in the germarium and proceeds posteriorly. Asterisk indicates germarium-vitellarium boundary. The four germaria are aligned from the cyst with shortest lengths.

arms in each cell and are presented in Table 2; the *X* chromosome is recognizable because it is associated proximally with the nucleolus, and one of the autosomal arms is distinguishable due to its association with the structure termed the blob (Figure 13, CARPENTER 1975a). The other three major arms have no unique distinguishing characteristics; they are presented by relative length with no intention to imply identity. Lengths of synaptonemal complex are presented graphically in Figure 2 for the *X* chromosome from telomere to point of entry into the nucleolus; where lengths are available from both four-ring-canal cells the average is plotted. The four germaria are aligned from the cyst of minimal length.

It can be seen from Figure 2 and Table 2 that the bivalent and total length of SC increases from mid-zygotene to pachytene, then decreases to approximately half that of the maximum. Minimum length is followed by a second increase. Decrease in length is accompanied by increase in thickness of SC (top to bottom; Figure 4*s*) and its associated chromatin, and the second increase in length is accompanied by a decrease in thickness; the changes in thickness are graphically presented in Figure 3. The most reasonable mechanism for the shortening and thickening involves reorganization of synaptonemal complex components and chromatin, accompanied by some loss of SC material; thus the SC appears not to be a rigid, immutable structure (*cf.*, CARPENTER 1975a).

It should be noted that the method of presentation of Figure 2 entails two unwarranted biological assumptions, to wit: that the inter-cyst temporal interval is constant both within and between germaria, and that the presumably continuous process of SC length change (and hence the remaining numerous other developmental parameters) was stopped at the same points in the various

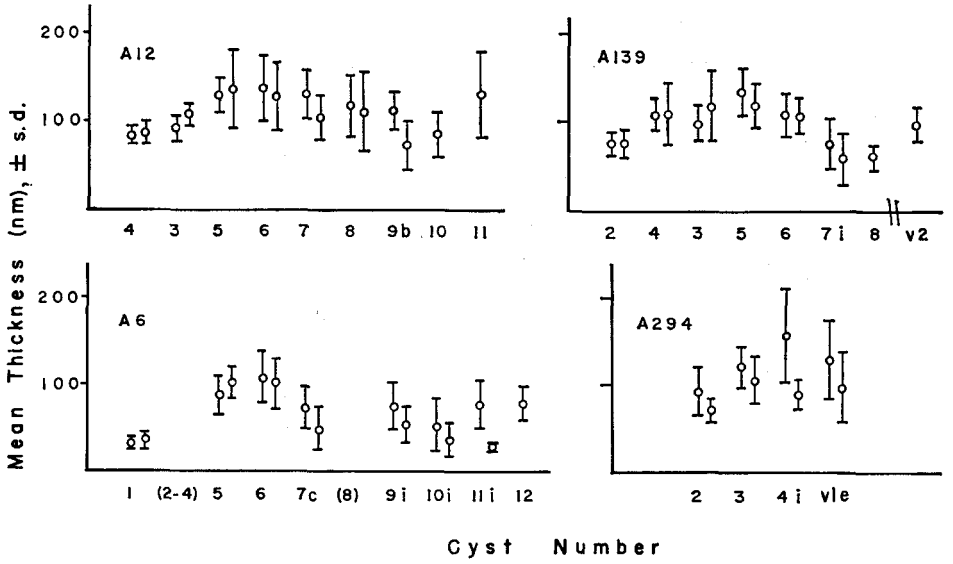


FIGURE 3.—Thickness of euchromatic synaptonemal complex as a function of developmental age of cyst. Heterochromatic synaptonemal complex is $\leq$ 75 nm thick.

germaria by the fixation. The latter assumption is, of course, unlikely; but simple abscissa shifts give a single sequence of lengths only if the former assumption is valid. Simple abscissa shifts do not give a smooth sequence for the entire data; however, a smooth sequence can be obtained from these data if the inter-cyst interval within germaria is considered to be variable (see Figure 9).

The model of germarium dynamics proposed by KING (1970) assumes that the inter-cyst interval is constant and that this interval is generated by the timed, sequential division of the stem cells. Recent evidence indicates that the stem cells frequently divide in bursts, rather than invariably sequentially (SCHÜPBACH, WIESCHAUS and NÖTHIGER 1978; WIESCHAUS and SZABAD 1979; the three sequential dying cysts in germarium A6 may well be the consequence of such a burst from a defective stem cell). Therefore, the assumption that the intercyst interval is constant needs to be re-examined. In order to measure the intercyst interval, one needs a measurable process that proceeds at a constant rate; insofar as the length changes of the SC meet these criteria (and it is certainly reasonable to assume that they do), then the data in Table 2 and Figure 2 indicate that the inter-cyst interval is not constant either within or between germaria.

All four completely analyzed germaria clearly show the same pattern and magnitudes of length changes; such changes therefore appear to be typical of Drosophila female pachytene (CARPENTER 1975a).

*Recombination nodules*

*Morphology*: Recombination nodules in Drosophila have been described as dense, spherical structures located adjacent to and between the chromatin of the

TABLE 3

*Numbers of ellipsoidal (E), spherical (S), and intermediate (I) recombination nodules in the nuclei of the various cysts in the four germaria*

| | A12 cysts | E | S | | A139 cysts | E | S | | A6 cysts | E | S | | A294 cysts | E | S |
|---|---|---|---|---|---|---|---|---|---|---|---|---|---|---|---|
| | 4,3 | 0 | 0 | | 2,4 | 0 | 0 | | 1–4 | 0 | 0 | | | | |
| | 5a | 3 | 0 | | 3i | 0 | 0 | | 5c | 2 | 0 | | 2h | 0 | 0 |
| | b | 4 | 0 | | a | 0 | 0 | | d | 1 | 0 | | e | 2 | 0 |
| op | 6a | 1 | 3 | op | 5i | 2 | 3 | op | 6d | 5 | 1 | | 3i | 6 | 0 |
| | b | 0 | 3 | | a | 2 | 4 | | i | 7 | 1 | | e | 8 | 1 |
| | 7a | 0 | 5 | | 6a | 1 | 2+1I | | 7c | 0 | 2 | op | 4i | 2 | 5+1I |
| | b | 0 | 4 | | i | 1 | 3 | | i | 0 | 3 | | e | 2 | 3 |
| | 8a | 0 | 2 | | 7a | 0 | 5 | | 8 | Necrotic | | | v1e | 1 | 4 |
| | b | 0 | 3 | | i | 0 | 3 | | | | | | i | 0 | 5 |
| | 9a | 0 | 3 | | 8a | 0 | 3 | | 9i | 0 | 3 | | | | |
| to NC | b | 0 | 3 | NC | i | NP | | | c | 0 | 5 | | | | |
| | 10a | 0 | 2+ | | v1a | 0 | (1+) | | 10c | 0 | 2 | | | | |
| | | | | | | | | | i | 0 | 5 | | | | |
| | 11a | 0 | (1+) | | v2a | 0 | 1 | | 11e | 0 | 4 | | | | |
| | | | | | | | | to NC | i | 0 | 4 | | | | |
| | | | | | | | | | 12a | 0 | 0 | | | | |

op = initiation of organellar passage; to NC = to nurse cell; NP = not photographed.

two homologues, above and adjacent to the central element of the synaptonemal complex. The total numbers of nodules per nucleus and their locations along the euchromatic portion of the bivalent arms correspond quite closely to the numbers and locations of genetically detected exchange events, suggesting the possibility that the recombination nodule performs a role(s) in the recombination process (CARPENTER 1975b).

Recombination nodules of the typical spherical morphology have been observed in the nuclei of the germaria A12, A139, A6, and A294; the numbers of such nodules are presented in Table 3 (for A12 see CARPENTER 1975b). Moreover, a second type of nodule—herein termed ellipsoidal in distinction to the spherical nodules previously reported—has also been observed in these nuclei; the numbers of ellipsoidal nodules are also presented in Table 3.

That "spherical" nodules are roughly spherical in shape is indicated by the fact that they present an approximately round profile regardless of the plane of sectioning (Figure 4k-r). Ellipsoidal nodules, on the other hand, present different profiles in different planes of sectioning; when the synaptonemal complex is in a cross-sectional series, then the nodule presents a round profile adjacent to the central element that extends through several (up to 4) sections (Figure 4b-e, f); when the synaptonemal complex is in frontal or sagittal section, then the nodule presents an elliptical profile along the central element (Figure 4g, h, i, j); when the synaptonemal complex is in nonorthogonal section, the shape of the nodule is frequently difficult to establish. Taken together, the three types of orthogonal views require that the "ellipsoidal" nodules be in fact ellipsoidal (or cylindrical) in shape, with the long axis of the ellipsoid parallel to the longitudinal axis of the synaptonemal complex (Figure 4s).

That there are two distinct types of nodules is shown in plots of measurements of spherical and ellipsoidal nodules (Figure 5). Although length of ellipsoidal nodules varies considerably (Figure 5a), diameter (width or height) is nearly constant; ellipsoidal nodules as a class have an average diameter of 34.9 ± 5.0 nm—quite close to the width of the central element (32.1 ± 2.7 nm, CARPENTER 1975a)—but variable length. For spherical nodules, on the other hand, even though there is quite a range in overall size, diameter and length are approximately equal. Thus, ellipsoidal and spherical nodules form two distinct populations in plots of length *vs.* diameter (measurements taken from frontal and sagittal views, Figure 5a) and also separate, but less distinct, populations in plots of width *vs.* height (measurements from cross-sectional views, Figure 5b). Measurements from nonorthogonal views, excluded from Figures 5a and 5b, are consistent with the existence of two distinct populations.

The relationship between ellipsoidal and spherical nodules is not obvious. They do not appear to differ in substructure (Figures 4b-r), and they are both centered above the central element of the SC. However, they differ not only in shape but also in numbers per nucleus (Table 3), distribution along the bivalent arms (see below), and time of occurrence (Table 3).

Ellipsoidal nodules typically are present one cyst before spherical nodules are first observed, then decrease dramatically in number in subsequent cysts. This

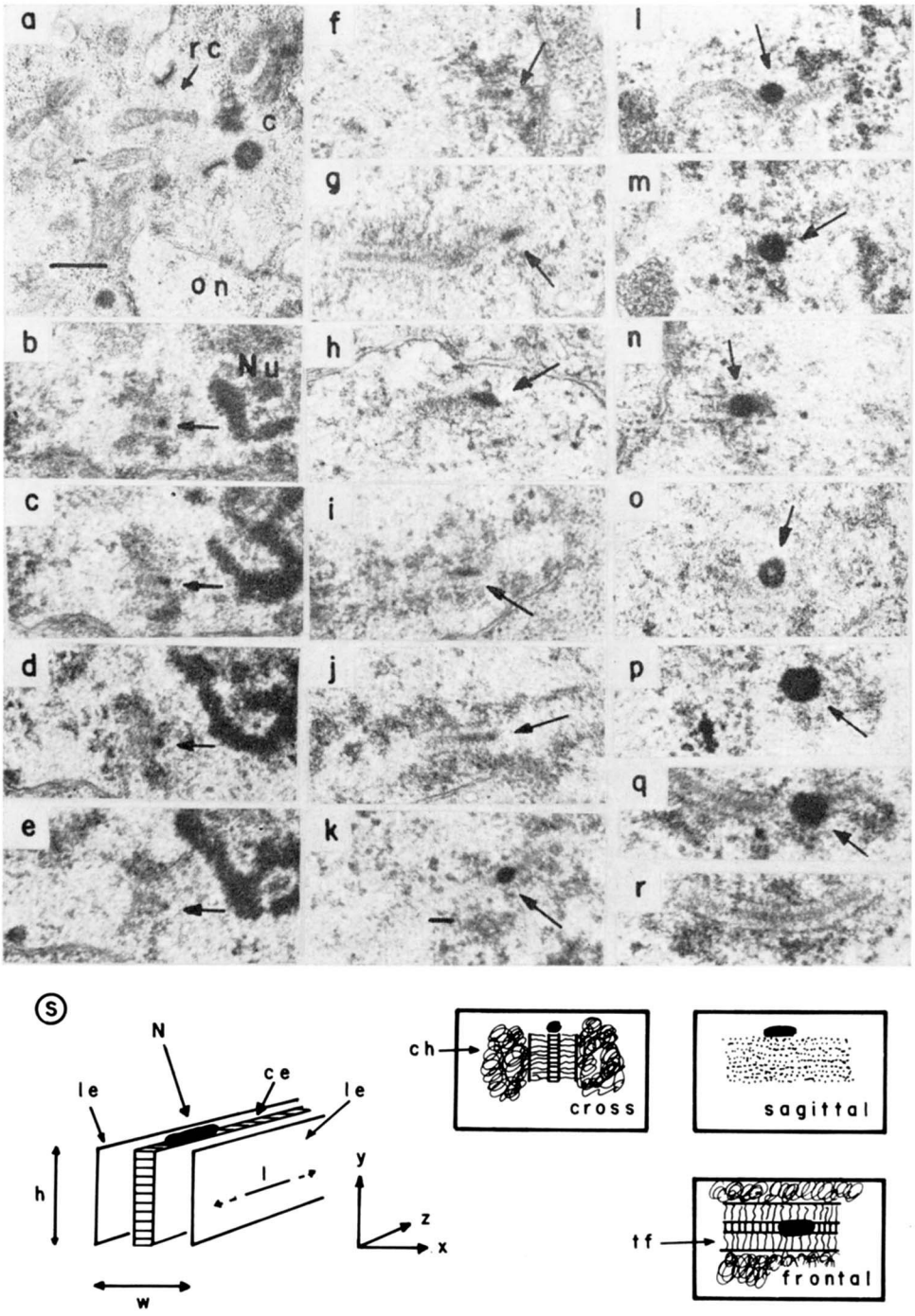


FIGURE 4.—Ellipsoidal and spherical recombination nodules. (a) Early organellar passage: *rc* ring canal, *on* pro-oocyte nucleus, *c* centriole. A139:5a. (b-e) Ellipsoidal nodule in cross sec-

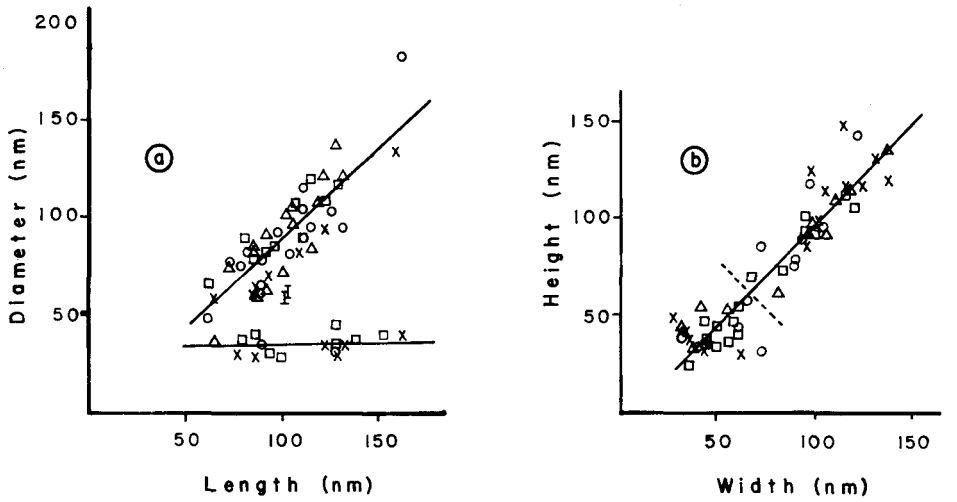


FIGURE 5.—Dimensions of recombination nodules. Symbols for germarium of origin are as in Figure 2. Lines are least-squares fits. Figure 5a: spherical (upper line) and ellipsoidal (lower line) nodules for which the adjacent SC has been sectioned in the frontal or sagittal plane. For spherical nodules, mean diameter = 91 nm, length = 101 nm, slope = 0.92; for ellipsoidal nodules, mean diameter = 35 nm, length = 106 nm, slope = 0.04. I = nodule of "intermediate" size; they have been excluded from these calculations. Figure 5b: spherical and ellipsoidal nodules for which the adjacent synaptonemal complex is in cross section. Dashed line indicates the (arbitrary) demarcation between ellipsoidal (below) and spherical (above). For spherical nodules, mean height = 101 nm, width = 102 nm; for ellipsoidal, mean height = 40 nm, width = 46 nm. Slope of line = 1.01.

temporal order is suggestive of a precursor-product relationship. However, if ellipsoidal nodules be precursors of spherical nodules, then nodules intermediate in size and shape would be expected; few possible intermediates were found. Two nodules, intermediate in both size (points "I" in Figure 5a; excluded from both least-squares calculations) and shape (roughly spindle-shaped) have been observed among those nodules sectioned in sagittal or frontal planes; both of these

---

tion: four consecutive sections. Arrow indicates nodule; *Nu* nucleolus. A6:6i. (f) Ellipsoidal nodule, cross section. A6:6i. (g,h) Two ellipsoidal nodules, slanting sagittal section. A294:4e, 3e. (i,j) Two ellipsoidal nodules, frontal section. A6:6d, 5c. (k) Spherical nodule, frontal section. A6:7c. (l) Spherical nodule, sagittal section. A6:9i. (m,n) Two spherical nodules, cross section. A6:9c, A294:4i. The nodule in n appears to be regionally decondensed, a phenomenon observed in seven of the 18 spherical nodules of germarium A294, perhaps correlated with the overall dehydration and chromatin decondensation observed in this germarium. (o) Spherical nodule, sagittal section. A139:7i. Print dodged to show apparent hollow core, a phenomenon occasionally observed in the larger spherical nodules. (p-r) Spherical nodule in frontal section, three consecutive sections. A6:10c. (s) Diagram of SC with an ellipsoidal nodule and the results of the three orthogonal planes of section. *h* height (= thickness), *w* width, *l* length, *N* nodule, *le* lateral element, *ce* central element, *ch* chromatin, *tf* transverse filaments. (A cross section is in the *xy* plane, sagittal is in the *yz* plane, and frontal is in the *xz* plane.) a × 15,600, bar = 0.5 μm; b-r × 29,500, bar (in k) = 0.1 μm.

nodules in fact occurred in nuclei containing both ellipsoidal and spherical nodules, an appropriate place for intermediates. Potential intermediates cannot be discerned when the nodule is seen in cross section, since the range of diameters of spherical and ellipsoidal nodules abut (Figure 5a) and shape variations along the length of the nodule cannot be discerned. The distribution of points in Figure 5b does give the impression of two clusters of sizes, with but few intermediates. Of the seven nodules intermediate in size between the smaller and the larger clusters in Figure 5b, four occur in nuclei that contain both ellipsoidal and spherical nodules (A12 cyst 6–1; A294 cyst 4–2; and A139 cyst 5–1) and three occur in nuclei whose remaining nodules are spherical (A12 cyst 7–2; cyst 8–1). However, average size (diameter) of spherical nodules does increase with increasing developmental age of cyst in all four germaria (Figure 6), although a wide range of sizes is found in any one nucleus, so that these nodules of intermediate cross-sectional sizes could represent either small ("young?") spherical nodules or a conformational intermediate between ellipsoidal and spherical morphologies.

*Distributions of spherical nodules along and among the bivalents*: Since the meanders of the synaptonemal complex, and hence the bivalents, have been reconstructed and measured in these nuclei, it is possible to determine where along the arms the various nodules are positioned. Figures 7g and h summarize the locations of spherical nodules in the four germaria, each of which exhibits the same overall pattern; for the purposes of comparative presentation, the synaptonemal complex length from telomere to euchromatic-heterochromatic juncture for each arm is normalized to one, and numbers of nodules are plotted by tenths of arms. As before (CARPENTER 1975b) with the smaller set of data from A12

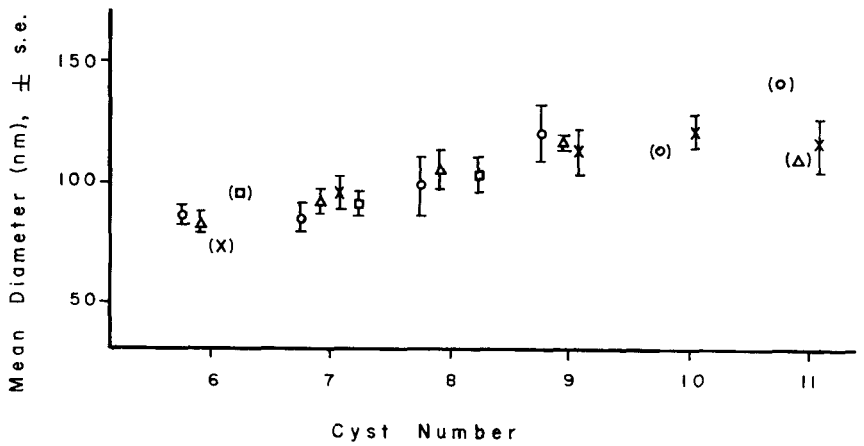


FIGURE 6.—Size of spherical nodules as a function of developmental age. Symbols for germaria and germarial alignment are as in Figure 2; cyst numbers are those of A12/A6. Parentheses enclose means based on only one or two nodules. Since spherical nodules are spherical (see Figure 5), the two measurements for each nodule were first averaged, then these average diameters were used to calculate means and standard errors of means.

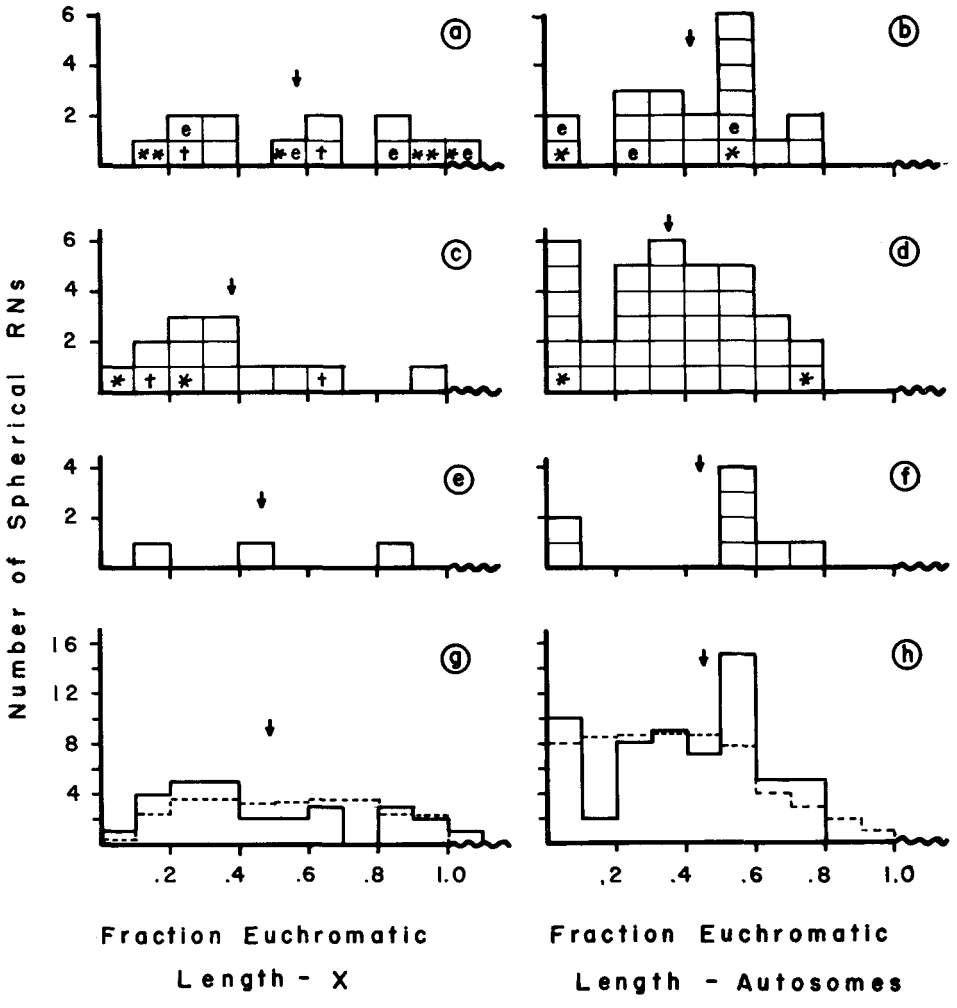


FIGURE 7.—Distributions of spherical nodules along the bivalent arms of the *X* chromosome and of the autosomes. (a,b) early = contemporaneous with ellipsoidal nodules (A12 cyst 6, A139 cysts 5 and 6, A6 cyst 6, A294 cysts 3 and 4); (c,d) middle = between early and late (A12 cysts 7 and 8, A139 cyst 7, A6 cysts 7, 9 and 10, A294 cyst v1); (e,f) late = oocyte determined (A12 cysts 9 and 10, A139 cysts 8 and v2, A6 cyst 11); (g,h) total. Arrow = mean, like symbols (*e.g.*, *,*) indicate the two positions of binodulate arms. Dashed lines in (g,h) indicate physical distributions of exchange events calculated from LINDSLEY and SANDLER (1977) normalized to the total number of nodules, e = bi (or tri) nodulate arm in which the other nodule(s) is ellipsoidal.

only, the distribution of locations of spherical nodules closely approximates the distribution of locations of exchange events.

Explicit comparisons between physical distribution of exchange sites and locations of spherical nodules are more meaningful if the *X* chromosome and the autosomes are considered separately, since the patterns differ quantitatively. Physical distribution of exchange sites have been calculated by many people over

the years; the most recent, complete compilation is that of LINDSLEY and SANDLER (1977, their Figure 1), which will be used here. Physical distributions of spherical nodules for the autosomes and for the *X* chromosome are presented in Figures 7g and h. Comparisons between the two types of distribution are restricted to gross aspects by low total numbers of nodules on the one hand and by limitations on the sizes of well-defined genetic intervals on the other. Within reasonable limits, exchange and nodule distributions show good concordance for both the *X* chromosome and the autosomes.

Exchange sites are uniformly distributed along most of the *X* euchromatin; there is a slight decrease in proximal regions and a dramatic decrease in the distal-most region (8% of the total length). Spherical nodules are also fairly uniformly distributed along the *X* chromosome; there is a paucity of nodules in the distal 10%, but the concordance between exchanges and nodules in a segment this short must be considered tentative because of the low total numbers of nodules.

There is essentially no exchange in the *X* heterochromatin; with but one exception, nodules are similarly restricted to the clearly euchromatic portion of the bivalent. The exceptional nodule appears to be located just on the heterochromatic side of the euchromatic-heterochromatic boundary, as judged by chromatin compactness; however, the SC adjacent to this nodule is more typical of that associated with euchromatin than that associated with heterochromatin in terms of morphology of components and thickness. It has been noted (CARPENTER 1975a; CARPENTER and BAKER 1974) that the transition between euchromatic and heterochromatic morphology of SC and chromatin is typically not abrupt, but rather occurs gradually over some distance; this nodule is located within the transition zone and therefore is not a clear exception to the otherwise exclusively euchromatic location of nodules.

Distributions of exchanges along the autosomal arms are more complicated, but if fluctuations in the coefficient of exchange for short intervals are ignored [as LINDSLEY and SANDLER (1977) point out, these fluctuations may be artifactual], then the broad pattern is that the coefficient of exchange is high and relatively uniform in the distal 60% of the euchromatin, low in the proximal 40% with decreasing amounts of exchange per unit length the more proximal the region, and zero in the proximal heterochromatin. The distribution of spherical nodules along the autosomes certainly follows this general pattern (Figure 7h) and in fact correlates rather well with the detailed pattern (LINDSLEY and SANDLER 1977, Figure 1) in that a sub-terminal dip is observed in both distributions. Terminal dips and sub-terminal peaks are also observed in both distributions—there are but three nodules in the ultimate 5%, seven in the penultimate 5%. Thus, total spherical nodule bivalent distributions correspond quite closely to the distribution of exchange sites.

Moreover, the distribution of numbers of spherical nodules per bivalent arm is not random but instead closely approximates the distribution of numbers of exchanges per arm. Among the nine nuclei with four or more total spherical nodules, there were eight arms with no sperical nodules ($N_o$), 32 with one

($N_1$), and five with 2 ($N_2$), for an avearge of 0.93 nodules per arm; the expected numbers of arms with zero, one, and two or more nodules is 17.7, 16.5 and 10.7, based on the Poisson distribution. The observed numbers per arm differ significantly from the random expectation ($\chi_1^2 = 23$, $P<<0.01$). In fact, for these nuclei the distribution of number of nodules per arm is exceedingly close to the distribution of the number of exchanges per arm (expected numbers 6.3, 32.8, and 5.8, from LINDSLEY and SANDLER 1977; $\chi_2^2 = 0.59$, $P>0.7$).

*Temporal changes in nodule distributions*: Do nodule positions change with time? In order to examine possible temporal differences in distribution, cysts with spherical nodules have been assigned to three groups: early = spherical and ellipsoidal nodules co-exist (A12 cyst 6, A139 cyst 5 and 6, A6 cyst 6, A294 cysts 3 and 4); late = oocyte determined—SC of other cell with four ring canals no longer reconstructable (A12 cyst 9, A139 cysts 8 and 9, A6 cyst 11); and middle = the rest— this group includes some nuclei that are presumably determined to revert to nurse-cell function (and one that is on the way) as recognized by centriolar accumulation in the other four-ring-canal cell (A12 cysts 7 and 8, A139 cyst 7, A6 cysts 7, 9, and 10, A294 cyst v1). Data are presented in Figure 7a-f; mean nodule positions are indicated by arrows. Although the distributions differ slightly at the different times, the differences are neither large nor consistent, and therefore the conservative conclusion is that, if there are temporal differences in nodule position, they are relatively slight.

The number of nodules per nucleus, on the other hand, does vary with developmental age of cyst (Table 3); there are fewer nodules per nucleus in early and late cysts than in middle ones, implying asynchrony of appearance/disappearance. It is not possible from the data at hand to determine the average temporal duration of spherical nodules, and therefore the maximum number observed per nucleus (six) may be an underestimate of the number a nucleus may experience.

Asynchrony in appearance and disappearance of nodules also appears to be present at the level of individual bivalent arms. For nuclei older than the cysts with four or more nodules per nucleus, $N_1$:$N_2$ = 15:0 (30 arms total), whereas the ratio would be expected to be about 13:2 if disappearance of multiple nodules along an arm were concordant. Similarly, for the 11 nuclei younger than or at the same developmental stage as those with four or more nodules, $N_1$:$N_2$ = 25:1 (55 arms total); the ratio would be expected to be about 23:3 if appearance of multiple spherical nodules along an arm were synchronous. Although the data are few, the relative paucity of $N_2$ bivalent arms before and after the maximum numbers of spherical nodules per nucleus suggests that the appearance and disappearance of multiple nodules per arm may not be synchronous. However, there is a caveat with respect to appearance: three of the 25 $N_1$ arms from the earlier nuclei had, in addition to the spherical nodule, one or more ellipsoidal nodules; if (some of) the ellipsoidal nodules are spherical nodule precursors, then the $N_1$:$N_2$ ratio becomes 22:4, a ratio not inconsistent with synchrony of appearance.

Desynapsis (disappearance of SC and concomitant decondensation of chromatin) typically begins in the pro-nurse cell while some nodules remain. Those nodules that are present are associated with residual intact stretches of SC, as

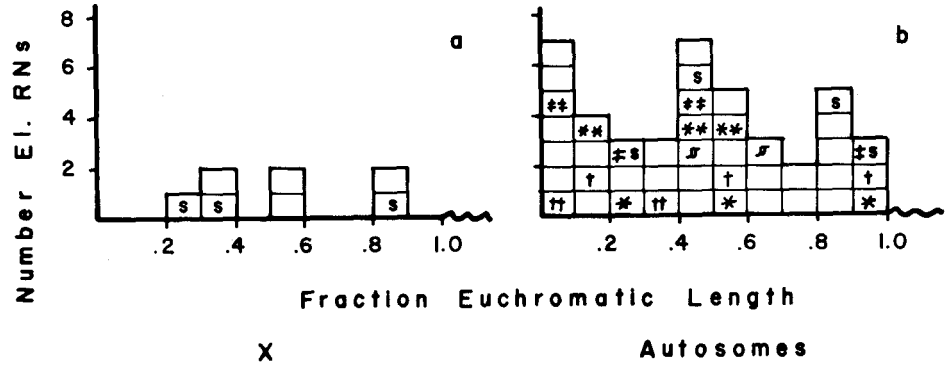


FIGURE 8.—Distributions of ellipsoidal nodules along the bivalent arms of the *X* chromosome and of the autosomes. Like symbols (*e.g.*, *,*,*) indicate the two or three positions in bi- or tri-nodulate arms; s = bi- (or tri-) nodulate arm in which the other nodule(s) is spherical.

are nodules present at diplotene in Sordaria (ZICKLER 1977) and Neurospora (GILLIES 1979), although here there are many segments of non-nodulated SC. In the oocyte, however, the SC remains intact for some time after all nodules have disappeared.

*Distribution of ellipsoidal nodules*: The locations of ellipsoidal nodules along the autosomal arms differ from that of spherical nodules (Figure 8) (there are too few *X*-associated ellipsoidal nodules for comparison). The most striking difference involves the very proximal regions; 8/42 (19%) of the ellipsoidal nodules fall within the proximal 20% of the euchromatin, whereas 0/61 of the spherical nodules were found in the proximal 20%. In general, ellipsoidal nodules appear to be rather uniformly distributed along the euchromatic length.

The maximum number of ellipsoidal nodules per nucleus in this sample (eight) is higher than that of spherical nodules (six), and the numbers per arm are also higher. There are five nuclei with four or more total ellipsoidal nodules; these five give $N_0 = 5$, $N_1 = 13$, $N_2 = 4$, $N_3 = 3$, for a mean of 1.20 nodules per arm. (Poisson expectations for these nuclei are: $N_0 = 7.5$, $N_1 = 9.0$, $N_2 = 5.4$, $N_{\geq 3} = 3.0$; $\chi_1^2 = 2.8$, $P > 0.05$; thus, the hypothesis that the interchromosomal distribution of ellipsoidal nodules is random cannot be rejected.) Most striking is the large proportion of bivalent arms with multiple ellipsoidal nodules; no instances of arms with three spherical nodules have been observed. Spherical nodules correspond to reciprocal exchange events in numbers per nucleus, numbers per arm, and location along the *X* chromosome and the autosomes; ellipsoidal nodules differ from both spherical nodules and reciprocal exchange events in all of these parameters. However, neither exchange nor spherical or ellipsoidal nodules occur in the proximal heterochromatin.

*Interference distances*: That reciprocal exchange events exhibit positive chiasma interference in Drosophila is well established; for the *X* chromosome, the two exchanges in an $E_2$ tetrad are, on average, separated by 45% of the euchromatin (CHARLES 1938). Inspection of Figures 7 and 8 suggests that spheri-

TABLE 4

*Interference distances for multiply-nodulate arms as proportion of total euchromatic length of the arm*

| Germarium | E-E | S-S | S-E | E-E-E | E-S-E | E-S-S |
|---|---|---|---|---|---|---|
| A12 | 0.40 | 0.77 | | | | |
| | | 0.65 | | | | |
| A139 | | 0.48 | | | | |
| | | 0.47 | | | | |
| A6 | | 0.23 | 0.63 | 0.29, 0.38 | | |
| | | | 0.48 | 0.37, 0.11 | | |
| A294 | 0.27 | 0.45 | 0.13 | 0.40, 0.41 | 0.03, 0.67 | 0.30, 0.47 |
| | 0.23 | | 0.76 | | | |
| $\bar{x} \pm$ s.e. | 0.30±0.05 | 0.51±0.08 | 0.50±0.14 | 0.33±0.05 | | |
| Expectation if no interference | 0.33 | 0.33 | 0.33 | 0.25 | | |

S = spherical nodule; E = ellipsoidal nodule.

cal nodules show interference, but that ellipsoidal nodules do not; it is possible to test this impression although the numbers of multiply-nodulate arms are too few for definitive conclusions.

If $n$ points be placed at random on a line of unit length, the average distance between adjacent points $= 1/(n+1)$. Therefore, positive interference of nodules is indicated for $N_2$ arms if the average internodule distance is greater than 0.33, for $N_3$ arms if the average internodule distance is greater than 0.25.

The data are presented in Table 4; spherical-spherical and spherical-ellipsoidal pairs do appear to show interference (since single spherical nodules are in fact not uniformly distributed along the euchromatin, the expected internodule distance is actually somewhat less than 0.33). Ellipsoidal nodules, however, exhibit little if any interference.

## DISCUSSION

### *Developmental progressions*

The more extensive data presented here on the organization of the *Drosophila melanogaster* germarium serve to confirm and extend the earlier observations (CARPENTER 1975a, b) on temporal progressions of events within the germarium. The order of cysts within the germarium appears to reflect order with respect to developmental ages of cysts in that the spatial order corresponds to sensible progressions of a number of intra-cyst events: formation of SC and its subsequent changes in length and thickness, initiation and increase in the amount of organellar passage, appearance and disappearance of recombination nodules, determination of oocyte and the accompanying reversion of the other four-ring-canal cell to nurse cell morphology, and finally karyosome formation. It is unlikely that there would never be temporal disorder of cysts, especially since the first

(anterior) several 16-cell cysts are typically essentially abreast with only slight regions of overlap from which the anterior-posterior ranking can be determined, but such disorder appears to be rare.

It is striking that none of the above developmental parameters correlate with absolute germarial position, with the possible exception of SC formation. Zygotene (SC formation not yet complete) nuclei have been found only in the anterior region where cysts are abreast or nearly so [roughly equivalent to KING's (1970) region 1], although the zygotene cyst may be the first (youngest-A6, A305) or there may be intervening pre-zygotene cysts (A12, A139, A294, A54, A84, A287). The point of minimum SC length and maximum thickness ranges from mid-germarium [at the point where the cysts first extend fully across the diameter of the germarium, roughly equivalent to the anterior end of KING's (1970) region 2—(A12 cyst 7, A6 cyst 7)] to the posterior end of the germarium (A294 cyst 4). Initiation of organellar passage shows a similar variability, occurring one cyst before minimum SC length in A12, A139, and A6 and at minimum length in A294. Clear determination of oocyte (other nucleus unreconstructable due to extensive disappearance of SC) occurs in the posterior region of the germarium in A12 (cyst 9), A139 (cyst 8) and A6 (cyst 11), but not in A294 (all germarial cysts fully reconstructable). Condensation of oocyte chromatin into the karyosome has occurred by the last germarial cyst [=stage 1 of vitellarial sequence in KING's nomenclature] in A6 but not in A12, A294, or A139 (for A139 the second vitellarial cyst was photographed and reconstructed; the karyosome state had been attained).

It is, however, even more striking that all of the germaria show the same progressions not only of individual intracyst events but also of correlations between the various events, indicating that the various parameters examined do reflect a basic developmental sequence. This sequence is visualized in Figure 9, in which the cysts from the four germaria are interdigitated by the criterion of SC length; the events of initiation of organellar passage, oocyte determination, and presence of recombination nodules are simultaneously brought into almost perfect register. Since the various monitored events appear to reflect a common temporal (developmental) sequence, the presence/absence of one event can be used to predict the presence/absence of another.

One of the purposes of this extensive analysis of germarial events in wild type was to discover events that mark the beginning and the end of the pachytene period in wild type during which nodules are found in order to ascertain whether mutants defective in recombination alter the number of nodules. The first appearance of spherical nodules corresponds quite closely to the initiation of organellar passage (Table 3 and Figure 9), and therefore this event can be used to predict the beginning of the spherical nodule period. Complete disappearance of nodules occurs shortly after the attainment of the oocyte-nurse cell dichotomy, and therefore this event can be used to indicate a point near, but before, the end of the spherical nodule period. For the four wild-type germaria, there are a total of 100 spherical nodules in 31 nuclei for an average of 3.23 nodules per nucleus; for the oocytes and pro-oocytes between the events of initia-

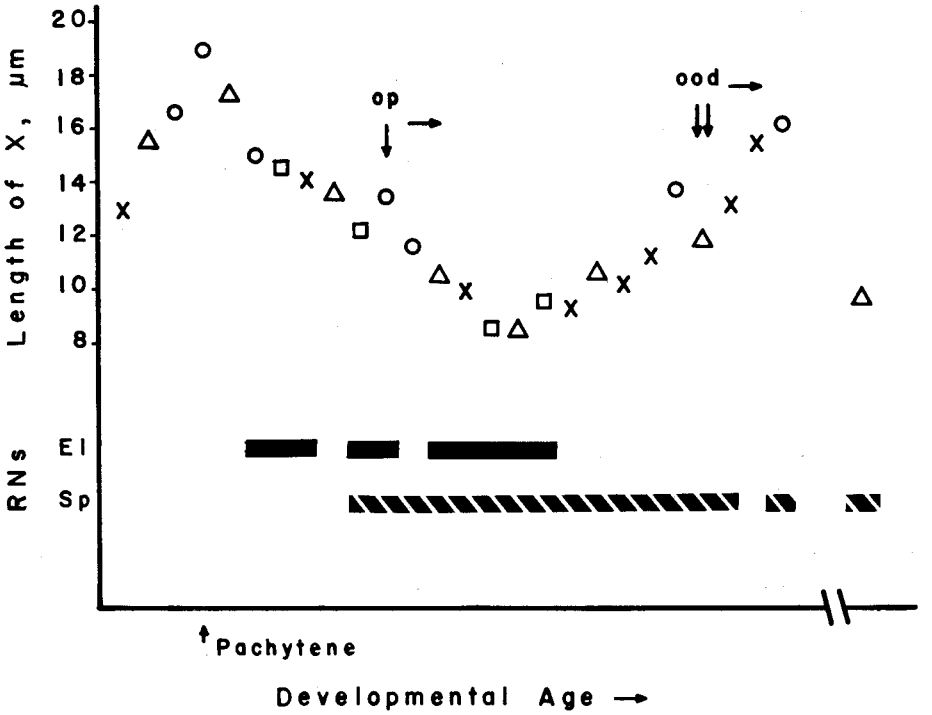


FIGURE 9.—Composite developmental sequence of SC length, organellar passage (= op), oocyte determination (= ood), and presence of ellipsoidal (El) and spherical (Sp) recombination nodules in the four germaria. Germarial symbols as in Figure 2: inter-cyst interval assumed to be variable.

tion of organellar passage and oocyte determination (inclusive) there are 91/27 = 3.37. The events of initiation of organellar passage and oocyte determination, therefore, span most of the spherical nodule period and provide marker events delimiting a developmental period during which an average of 3.37 ± 0.24 (s.e.) nodules per nucleus are predicted to occur.

Virtually all (48/50) of the ellipsoidal nodules are found in the three cysts per germarium spanning the initiation of organellar passage. Ellipsoidal nodules are therefore predicted to be present around the time of this event, but a discrete developmental period during which ellipsoidal nodules are present cannot be delimited by reference to this one event since the inter-cyst interval does not appear to be constant (see above and Figure 9).

*Role of recombination nodules*

Spherical recombination nodules (the unqualified recombination nodules of CARPENTER 1975b) in Drosophila correlate closely with reciprocal exchange events in number per nucleus, number per bivalent arm, distribution along the bivalent arms, and presence and magnitude of chiasma interference, and therefore appear to indicate the site of exchange (CARPENTER 1975b). Similar corre-

lations between numbers of exchanges (or chiasmata) and nodules and, at least roughly, chromosomal locations, have been reported in *Saccharomyces cerevisiae* (BYERS and GOETSCH 1975), *Sordaria macrospora* (ZICKLER 1977), and *Neurospora crassa* (GILLIES 1979); positional correlations have been reported in *Rattus norvigicus* (MOENS 1978). In addition, nodules have been noted in all thorough studies and in many surveys of eukaryotes known or reasonably expected to be recombinationally proficient (SCHRANTZ 1970; ZICKLER 1973; H. FLETCHER personal communication; STORMS and HASTINGS 1977; BOGDANOV 1977; MOSES, RUSSELL and CACHEIRO 1977; MOSES 1977a, b, and personal communication; CARMI *et al.* 1978; GOLDSTEIN and TRIANTAPHYLLOU 1978; RASMUSSEN, cited in GILLIES 1979); structures analogous to recombination nodules in other organisms appear not to be present in the recombination-deficient *Bombyx mori* female (RASMUSSEN 1976, 1977). The number and chromosomal distribution of nodules may well become the probe of choice for examining the amount and location of exchanges in organisms lacking both cytologically tractable diakinesis and extensive genetics, just as reconstruction of the SC has permitted examination of synaptic configurations in all organisms (MOENS and PERKINS 1969).

Recombination nodules show some variability between the different species so far examined in morphology (fungal nodules are typically broad ellipsoids, rat nodules may be spherical, elongated along the longitudinal axis of the synaptonemal complex, or elongated across the central space), in position relative to the synaptonemal complex (fungal nodules are within the central space and include —or replace—the central element; nodules in rat and Drosophila are external to the complex itself), and in time of occurrence (in Sordaria and Neurospora nodules are observed from zygotene to diplotene, in Drosophila they are seen only during mid-pachytene, and in Meloidogyne only during late pachytene-diplotene). Although too few organisms have as yet been examined in detail for the establishment of categories, there appear to be consistent differences between the nodules of fungi and higher eukaryotes in association with the SC and time of occurrence.

Nodules of two size classes have been reported in Chlamydomonas (STORMS and HASTINGS 1977) and Neurospora (GILLIES 1979), although it seems doubtful on morphological and positional grounds whether the larger class of Chlamydomonas "nodules" correspond to nodules observed in other organisms. In Neurospora, the ranges in size of the two classes overlap so extensively that unequivocal classification is not possible (GILLIES 1979). There do appear to be two distinct size classes of nodules in Drosophila (here named ellipsoidal and spherical), but the relationship between them is unclear.

There are three possibilities for the relationship between ellipsoidal and spherical nodules: (1) they may be unrelated, (2) ellipsoidal nodules may be precursors of spherical nodules, or (3) they may perform similar, but not identical, functions. Although it is possible that ellipsoidal and spherical nodules might be unrelated structures, the similarities in general morphology, association with the synaptonemal complex, and sequential time of appearance make this unlikely.

It is entirely possible that ellipsoidal nodules are precursors of spherical

nodules, as indicated by their sequence of appearance and by the observation of two possible intermediates. If so, however, then there are several obligate corollaries. The maximum numbers of ellipsoidal nodules observed per cell exceeds that of spherical; therefore not all ellipsoidal nodules become spherical nodules. This corollary is also required by the differences in numbers per arm and distribution along the arms. Since, in the present data, ellipsoidal nodules are distributed uniformly along the euchromatic portion of the bivalents and spherical nodules are not, then if ellipsoidal nodules are precursors of spherical, there must be a process that determines which ellipsoidal nodules develop into spherical, and this process must be responsible for nonrandom distributions of nodules (1) between chromosomes, (2) along chromosome arms, and (3) relative to one another (interference).

Alternatively, a consideration of the current knowledge of the process of recombination raises the possibility that the two types of nodules mediate different types of events. In Drosophila, as in other organisms (see reviews by FINCHAM 1970; FOGEL and MORTIMER 1971; STADLER 1973; HASTINGS 1975), reciprocal events—which produce crossover chromatids and exhibit interference—represent only approximately half of the total recombinational events; nonreciprocal events (gene conversion)—which do not produce crossover chromatids and do not exhibit interference—represent the other half (see, for example, CHOVNICK *et al.* 1970; BALLANTYNE and CHOVNICK 1971). Spherical nodules and reciprocal events correspond in numbers per nucleus and per arm, distribution along arms, and presence of interference; ellipsoidal nodules do not correspond with reciprocal events for these parameters, but do correspond with conversion events in that both show little or no interference and both are relatively more frequent than reciprocal events/spherical nodules in proximal regions (GREEN 1975; SINCLAIR 1975). It is, therefore, possible that spherical nodules mediate reciprocal events (which may, of course, be accompanied by conversion at the site of the event), whereas ellipsoidal nodules mediate only nonreciprocal events (conversion without exchange of flanking markers).

Current models of the process of recombination at the DNA level assume that reciprocal recombination and nonreciprocal events (gene conversion only) occur by the same process, the outcomes differing only in which of two alternative states an intermediate is in when the irreversible next step in the process occurs (MESELSON and RADDING 1975, for example). The hypothesis that recombination nodules are instrumental in the recombination process itself (CARPENTER 1975b) has been criticized on the grounds that the maximum numbers of spherical recombination nodules per nucleus equals the number of reciprocal events, but is only half that of the total events under such models (HOLLIDAY 1977; MOENS 1978). There are a number of possible explanations for the discrepancy between maximum number of nodules and total recombination events: (1) recombination nodules may be sufficiently ephemeral that the number present in a nucleus at any one time is a gross underestimate of the total number experienced during pachytene, (2) the assumption that reciprocal and gene conversion events are alternative outcomes of the same process may be false—the two types of events

might be generated by separate processes, and (3) the role of the recombination nodule might encompass only later (post-isomerization) aspects of reciprocal events. Any of these would account for the discrepancies in numbers although an exclusively post-exchange role in which nodule presence is dependent upon the prior existence of a reciprocal event (HOLLIDAY 1977, MOENS 1978) is excluded by results from recombination-defective mutants (CARPENTER, in preparation).

Since there are two morphological types of recombination nodules with different numerical and distributional properties in Drosophila, the possibility that the processes that generate reciprocal and nonreciprocal events are at least in some respects separate merits serious consideration. If ellipsoidal nodules are precursors of spherical, then the outcome at a site (reciprocal *vs.* nonreciprocal) must be determined after site choice (indicated by formation of ellipsoidal nodules), but before the actual isomerization event itself; after the outcome is determined (by a process that is responsible for the nonrandom distributions of spherical nodules/reciprocal events), ellipsoidal nodules at sites that will undergo (exclusively) reciprocal events develop into spherical nodules, whereas those at sites that will undergo (exclusively) nonreciprocal events remain ellipsoidal nodules. If ellipsoidal nodules are not precursors of sperical nodules, then the outcome at a site must be determined by or at the time of nodule formation; spherical nodules are at sites that will undergo (exclusively) reciprocal recombination, whereas ellipsoidal nodules are at sites that will undergo (exclusively) gene conversion. Although the data at hand do not discriminate between these two alternatives, the second is more appealing in that processes that are responsible for the nonrandom distributions of spherical nodules/reciprocal events may well be integral aspects of the function(s) of spherical nodules themselves. It should be noted that, under either formulation, the only recombinational step that must be different in the two processes is the presence/absence of isomerization itself; all other steps—heteroduplex formation, for example—may not only be common to both processes, but may be under the same enzymatic control.

The notion that there may be two types of recombination is not new (see reviews by FINCHAM 1970; FOGEL and MORTIMER 1971; STADLER 1973; HASTINGS 1975); the specific separation of the domains of the two types that is indicated here was first proposed by STADLER and TOWE (1971), stimulated by observations on intragenic recombination in Ascobolus (it should be noted that STADLER and TOWE use somewhat different terminology than that used here). Individual loci show highly significant departures from 50% conversion-associated crossing over (see, for example, the data summarized from several organisms by WHITEHOUSE and HASTINGS 1965); either the probability of isomerization on a Meselson-Radding type of model differs for different loci, or else there are two recombination processes that have different spatial distributions along the chromosomes. Thus, both cytological and genetic evidence are consistent with the hypothesis that there are two at least partially separate meiotic recombination processes in eukaryotes.

The diligence of GARNETT SLATTON, LORRAINE DELATOUR, WALTER CLYNE, and TODD PRICE

in printing and of LEILANI SHAFFER in taking micrographs is gratefully acknowledged. I thank MONTROSE MOSES, who very kindly shared his facilities for part of this work, and BRUCE BAKER for his critical comments.

*Note added in proof*: Due to poor reproduction of the electron micrographs, the author will supply photographic reproductions of Figures 1 and/or 4 upon request.

## LITERATURE CITED

BALLANTYNE, G. H. and A. CHOVNICK, 1971 Gene conversion in higher organisms: Non-reciprocal recombination events at the rosy cistron in *Drosophila melanogaster*. Genet. Res. **17**: 139–149.

BYERS, B. and L. GOETSCH, 1975 Electron microscopic observations on the meiotic karyotype of diploid and tetraploid *Saccharomyces cerevisiae*. Proc. Natl. Acad. Sci. U.S. **72**: 5056–5060.

BOGDANOV, Y. F., 1977 Formation of cytoplasmic synaptonemal-like polycomplexes at leptotene and normal synaptonemal complexes at zygotene in *Ascaris suum* male meiosis. Chromosoma **61**: 1–21.

CARPENTER, A. T. C., 1973 A meiotic mutant defective in distributive disjunction in *Drosophila melanogaster*. Genetics **73**: 393–428. ——, 1975a Electron microscopy of meiosis in *Drosophila melanogaster* females. I. Structure, arrangement, and temporal change of the synaptonemal complex in wild-type. Chromosoma **51**: 157–182. ——, 1975b Electron microscopy of meiosis in *Drosophila melanogaster* females. II. The recombination nodule—a recombination-associated structure at pachytene? Proc. Natl. Acad. Sci. U.S. **72**: 3186–3189.

CARPENTER, A. T. C. and B. S. BAKER, 1974 Genic control of meiosis and some observations on the synaptonemal complex in *Drosophila melanogaster*. pp. 365–375. In: *Mechanisms in Recombination*. Edited by R. F. GRELL, Plenum Press, New York.

CARMI, P., P. B. HOLM, Y. KOLTIN, S. W. RASMUSSEN, J. SAGE and D. ZICKLER, 1978 The pachytene karotype of *Schizophyllum commune* analyzed by three dimensional reconstruction of synaptonemal complexes. Carlsberg Res. Commun. **43**: 117–132.

CHARLES, D. R., 1938 The spatial distribution of crossovers in *X*-chromosome tetrads of *Drosophila melanogaster*. J. Genet. **36**: 103–126.

CHOVNICK, A., G. H. BALLANTYNE, D. L. BAILLIE and D. G. HOLM, 1970 Gene conversion in higher organisms: half-tetrad analysis of recombination within the rosy cistron of *Drosophila melanogaster*. Genetics **66**: 315–329.

DAY, J. W. and R. F. GRELL, 1976 Synaptonemal complexes during premeiotic DNA synthesis in oocytes of *Drosophila melanogaster*. Genetics **83**: 67–79.

FINCHAM, J. R. S., 1970 Fungal genetics. Ann. Rev. Genet. **4**: 347–372.

FOGEL, S. and R. K. MORTIMER, 1971 Recombination in yeast. Ann. Rev. Genet. **5**: 219–236.

FRASCA, J. M. and V. R. PARKS, 1965 A routine technique for double-staining ultra-thin sections using uranyl and lead salts. J. Cell Biol. **25**: 157–161.

GILLIES, C. B., 1972 Reconstruction of the *Neurospora crassa* pachytene karyotype from serial sections of synaptonemal complexes. Chromosoma **36**: 119–130. ——, 1975 The synaptonemal complex and chromosome structure. Ann. Rev. Genet. **9**: 91–109. ——, 1979 The relationship between synaptonemal complexes, recombination nodules and crossing over in *Neurospora crassa* bivalents and translocation quadrivalents. Genetics **91**: 1–17.

GOLDSTEIN, P. and A. C. TRIANTAPHYLLOU, 1978 Occurrence of synaptonemal complexes and recombination nodules in a meiotic race of *Meloidogyne hapla* and their absence in a mitotic race. Chromosoma **68**: 91–100.

GREEN, M. M., 1975 Conversion as a possible mechanism of high coincidence values in the centromere region of *Drosophila*. Molec. Gen. Genet. **139**: 57–66.

HASTINGS, P. J., 1975 Some aspects of recombination in eukaryotic organisms. Ann. Rev. Genet. **9**: 129–144.

HOLLIDAY, R., 1977 Recombination and meiosis. Phil. Trans. R. Soc. Lond. B. **277**: 359–370.

KING, R. C., 1970 *Ovarian Development in* Drosophila melanogaster. Academic Press, New York.

KOCH, E. A. and R. C. KING, 1966 The origin and early differentiation of the egg chamber of *Drosophila melanogaster*. J. Morphol. **119**: 283–304.

KOCH, E. A., P. A. SMITH and R. C. KING, 1967 The division and differentiation of *Drosophila* cystocytes. J. Morphol. **121**: 55–70.

LINDSLEY, D. L. and E. GRELL, 1968 *Genetic Variations of* Drosophila melanogaster. Carnegie Inst. Wash. Publ. No. 627.

LINDSLEY, D. L. and L. SANDLER, 1977 The genetic analysis of meiosis in female *Drosophila melanogaster*. Phil. Trans. R. Soc. Lond. B. **277**: 295–312.

MAGUIRE, M. P., 1972 The temporal sequence of synaptic initiation, crossing over and synaptic completion. Genetics **70**: 353–370.

MAHOWALD, A. P. and J. M. STRASSHEIM, 1970 Intercellular migration of centrioles in the germarium of *Drosophila melanogaster*. J. Cell Biol. **45**: 306–320.

MESELSON, M. S. and C. M. RADDING, 1975 A general model for genetic recombination. Proc. Natl. Acad. Sci. U.S. **72**: 358–361.

MOENS, P. B., 1978 Lateral element cross connections of the synaptonemal complex and their relationship to chiasmata in rat spermatocytes. Canad. J. Genet. Cytol. **20**: 567–579.

MOENS, P. B. and F. O. PERKINS, 1969 Chromosome number of a small protist: accurate determination. Science **166**: 1289–1291.

MOSES, M. J., 1968 Synaptinemal complex. Ann. Rev. Genet. **2**: 363–412. ——, 1969 Structure and function of the synaptonemal complex. Genetics **61**: s41–52. ——, 1977a Microspreading and the synaptonemal complex in cytogenetic studies. Chromosomes Today **6**: 71–82. ——, 1977b The synaptonemal complex and meiosis. pp. 101–125. In: *Molecular Human Cytogenetics*, ICN-UCLA Symp. VII. Edited by R. S. SPARKES, D. COMINGS and C. F. FOX, Academic Press, New York.

MOSES, M. J., L. B. RUSSELL and N. L. A. CACHEIRO, 1977 Mouse chromosome translocations: visualization and analysis by electron microscopy of the synaptonemal complex. Science **196**: 892–894.

NOVITSKI, E., 1964 An alternative to the distributive pairing hypothesis in Drosophila. Genetics **50**: 1449–1451.

RADU, M., R. STEINLAUF and Y. KOLTIN, 1974 Meiosis in *Schizophyllum commune*: chromosomal behavior and the synaptinemal complex. Arch. Microbiol. **98**: 301–310.

RASMUSSEN, S. W., 1974 Studies on the development of the synaptinemal complex in *Drosophila melanogaster*. Comp. Rend. Trav. Lab. Carlsberg **39**: 443–468. ——, 1975 Synaptonemal polycomplexes in *Drosophila melanogaster*. Chromosoma **49**: 321–331. ——, 1976 The meiotic prophase in *Bombyx mori* females analyzed by three-dimensional reconstructions of synaptonemal complexes. Chromosoma **54**: 245–293. ——, 1977 Chromosome pairing in triploid females of *Bombyx mori* analyzed by three-dimensional reconstructions of synaptonemal complexes. Carlsberg Res. Com. **42**: 163–197.

REYNOLDS, D. R., 1963 The use of lead citrate at high pH as an electron-opaque stain in electron microscopy. J. Cell Biol. **17**: 208–212.

SCHRANTZ, J.-P., 1970 Etude cytologique, en microscopie optique et électronique, de quelques Ascomycétes. I. Le noyau. Rev. Cytol. et Biol. vég. **33**: 1–100.

SCHÜPBACH, T., E. WIESCHAUS and R. NÖTHIGER, 1978 A study of the female germ line in mosaics of *Drosophila*. Wilhelm Roux Arch. Entwicklungsmech. Org. **184**: 41–56.

SINCLAIR, D. A., 1975 Crossing over between closely linked markers spanning the centromere of chromosome 3 in *Drosophila melanogaster*. Genet. Res. **26**: 173–185.

SMITH, P. A. and R. C. KING, 1968 Genetic control of synaptonemal complexes in *Drosophila melanogaster*. Genetics **60**: 335–351.

STADLER, D. R., 1973 The mechanism of intragenic recombination. Ann. Rev. Genet. **7**: 113–127.

STADLER, D. R. and A. M. TOWE, 1971 Evidence for meiotic recombination in Ascobolus involving only one member of a tetrad. Genetics **68**: 401–413.

STORMS, R. and P. J. HASTINGS, 1977 A fine structure analysis of meiotic pairing in *Chlamydomonas reinhardi*. Expl. Cell Res. **104**: 39–46.

WESTERGAARD, M. and D. VON WETTSTEIN, 1972 The synaptinemal complex. Ann. Rev. Genet. **6**: 71–110.

WHITEHOUSE, H. L. K. and P. J. HASTINGS, 1965 The analysis of genetic recombination on the polaron hybrid DNA model. Genet. Res. **6**: 27–92.

WIESCHAUS, E. and J. SZABAD, 1979 The development and function of the female germ line in *Drosophila melanogaster*. A cell lineage study. Develop. Biol. **68**: 29–46.

ZICKLER, D., 1973 Fine structure of chromosome pairing in 10 ascomycetes: meiotic and premeiotic (mitotic) synaptonemal complexes. Chromosoma **40**: 401–416. ——, 1977 Development of the synaptonemal complex and the "Recombination Nodules" during meiotic prophase in the seven bivalents of the fungus *Sordaria macrospora* Auersw. Chromosoma (Berl.) **61**: 289–316.

Corresponding editor: L. SANDLER